

Chapter 6

Commissioning and investigations with TFS

Beam particles interact via direct space charge fields and through the electromagnetic fields induced in the walls of the vacuum chamber and the environment surrounding the beam (see chapter 3).

The beam environment can be characterised by a longitudinal and transverse impedance. Transversely the beam starts a coherent oscillatory motion around its equilibrium orbit. Because of the resistivity of the walls, these forces may have such a phase as to reinforce the oscillations and lead to instabilities. This phenomenon is called transverse resistive wall instability.

Apart from coherent instabilities where collective oscillations of the beam center or the beam shape grow exponentially due to interaction with surrounding structures one has to worry about incoherent effects which tend to destroy a high intensity beam. Both, coherent and incoherent phenomena depend on the beam density. It is important to measure the beam and the beam environment properties relevant for stability in an accelerator ring. There are two basically different ways of observing a beam in an accelerator [25, 31, 33]:

a passive one in which the observer does not disturb the beam (Schottky spectra)

an active one in which the observer deliberately excites the beam to record its response (BTF – the beam transfer function)

The arrangement to measure a beam transfer function is shown in figure 6.1. The beam transfer function (BTF) is defined as the response of a beam to a small longitudinal or transverse excitation. The BTF reveals phenomena such as Landau damping, the coupling impedance, active feedback system, non-linear resonances and the action of cooling systems. The contribution of each phenomenon can be extracted from the BTF. Important beam and machine parameters can be obtained directly from the measurement, such as the momentum distribution, the tune, the chromaticity and emittance in much the same way as from the Schottky noise measurements. BTF measurements are therefore an important and powerful tool for diagnostics of coasting particle beams, complementary to Schottky diagnostics and superior in situations where the Schottky noise is weak.

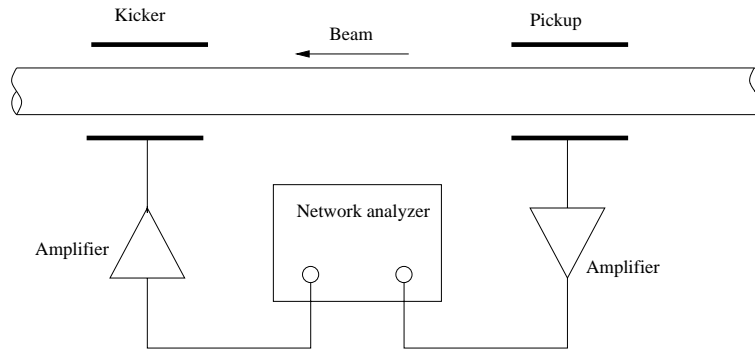


Figure 6.1: Arrangement to measure beam transfer function. The frequency sweep of the network analyser is set to cover one or several betatron sidebands.

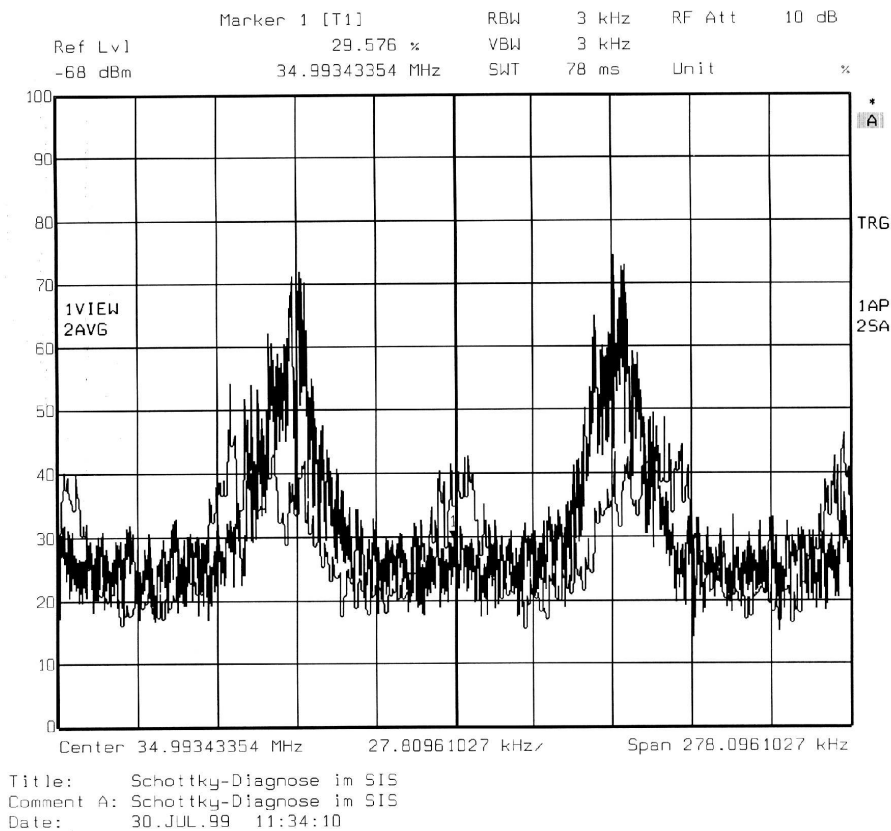


Figure 6.2: Vertical lower and upper betatron sidebands for the 163th harmonics of a $^{86}\text{Kr}^{34+}$ beam at the injection energy of 11.4 MeV/u. Due to coherent instabilities the transverse sidebands can increase.

An example of the transverse vertical coherent sidebands for the 163th harmonics of a $^{86}\text{Kr}^{34+}$ beam at the injection energy of 11.4 MeV/u is shown in figure 6.2. The Q – value was set to 3.29 and the measured Q – value was 3.26. This difference is due to an error between setting devices in the accelerator and controlling software. The Q – values correspond to the frequencies 60.11 kHz and 58.4 kHz, respectively. The measured centre frequency is 34.9934 MHz.

6.1 Environment diagnosis for TFS

In the following the measurements and diagnosis of components already installed in the SIS ring will be discussed. Because each component of the feedback system determine the parameters of the entire system it is important to know each component of the feedback system in detail. In summer 1999 the first series of measurements were carried out in the SIS because the new automatic feedback system is intended to be installed in this ring.

These measurements cover pickup measurements and the effects which can affect the efficiency of the TFS. During measurements described in the following a $^{86}\text{Kr}^{34+}$ beam at the injection energy of 11.4 MeV/u ($\beta = 0.16$) with $1.12 \cdot 10^8$ particles was used.

6.1.1 Pickup measurements

The goal of this measurement was to determine the frequency range and the resolution of the pickups together with the preamplifiers. Because the pickups already installed in the ring should sense the coherent oscillations, these measurements have to be done for better understanding the frequency range and corresponding sensitivity of the pickups.

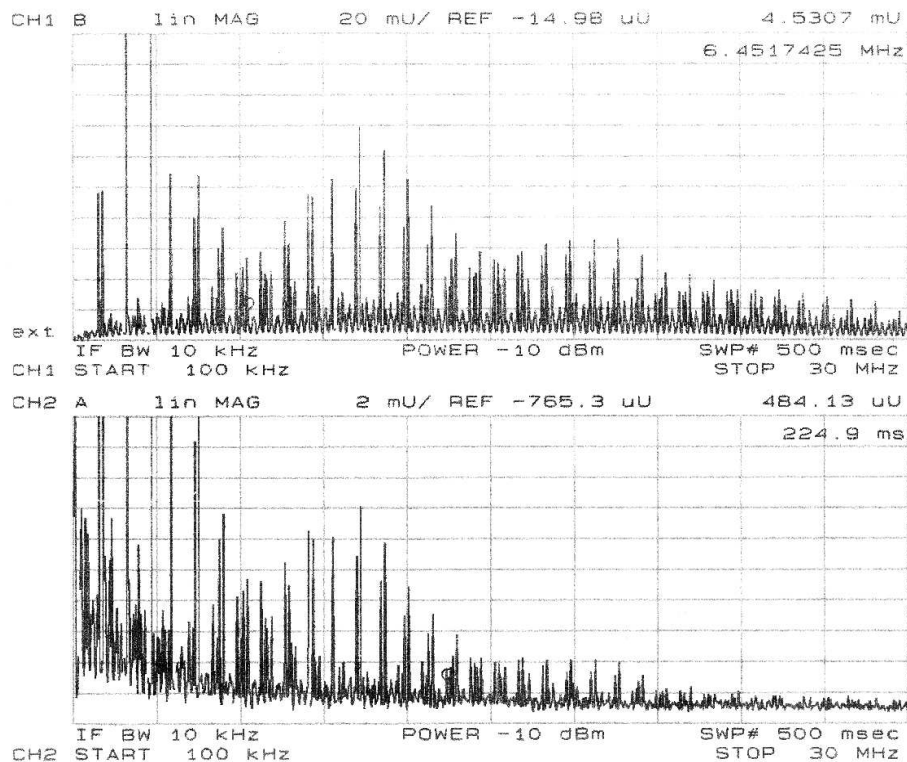


Figure 6.3: Pickup measurements in the frequency domain. The upper plot shows response of the Schottky pickup in the frequency range up to 30 MHz. The lower plot represents the same measurement with position pickup DX1.

Signals from the position pickups DX1 and DX5, and phase pickups DP1P and DP3P were measured. The comparison of the frequency spectrum of the position pickups and the Schottky pickups is useful for verification of the important parameters like the frequency range. The measurements were done under different conditions. At first, the

pickups were measured at the injection energy of (11.4 MeV/u) $\beta = 0.15$ and then at an extraction energy of (300 MeV/u) $\beta = 0.652$.

The verification of the DX1 pickup with the Schottky pickup can be seen in figure 6.3. The spectrum shown for the vertical plane is with kicker kicking in the same (vertical) direction at $\beta = 0.15$, the solenoid magnet of E-cooler was switched off and with connected extraction kicker. The result of these measurements was that during these tests the extraction kicker as well as the different energy levels had no influence on the frequency range of the pickups. From the measured spectra the conclusion can be drawn that the Schottky pickups are wideband devices and the position pickups are very sensitive in the low frequency range where the instabilities are expected.

During measurements on the pickup the coupling between both horizontal and vertical planes was observed and this will be discussed in the following section 6.1.2.

6.1.2 Effect of E-cooler

For purpose of the electron cooling system the solenoid magnet and toroids of the Electron-cooler were installed in the synchrotron. Because the solenoid can effect the frequency range or the resolution of the pickups it is necessary to investigate the effect of the solenoid magnet and toroids.

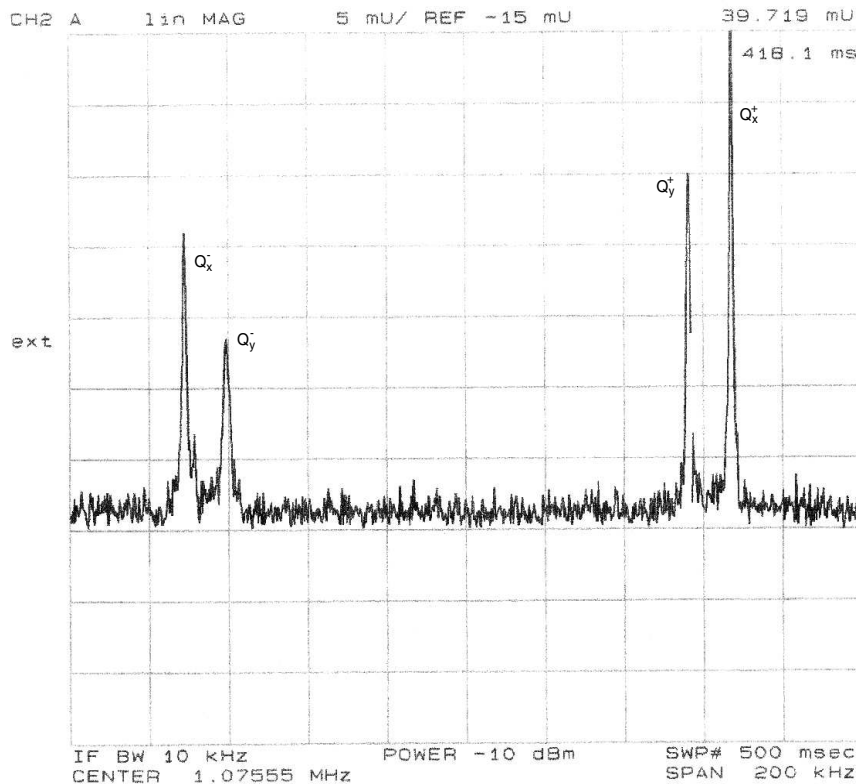


Figure 6.4: The effect of the solenoid magnet of the Electron-cooler on the 5th harmonic. Measured values of the tunes are $Q_y = 3.27$ and $Q_x = 4.32$.

The first measurement was carried out with following parameters for the SIS machine:

$$q_x = 0.29 \qquad q_y = 0.29 .$$

In order to measure the coupling between both vertical and horizontal planes the direction of the excitation was changed. Because the BTF was only used in one plane (vertical or horizontal) the sidebands had to be observed only in this “kicking” plane. The observed situation is shown in figure 6.4 for the 5th harmonic ($f = 1.0755$ MHz). The value of the tune Q_x^+ and Q_y^+ represent the vertical and horizontal sidebands both for fast waves, respectively. The value of the tune Q_x^- and Q_y^- represent the same for the slow waves. From this figure the measured fractional values of tune Q were:

$$q_y = 0.27 \qquad q_x = 0.32 .$$

In order to check the correctness of this calculations a value of $Q_y = 3.35$ was set far away from the normal machine tune of $Q_x = 4.29$. The measurement done with this set-up had shown that the solenoid magnet of the Electron-cooler causes a coupling between transverse and vertical planes. That means that the operation of the TFS together with electron cooling can be influenced by the solenoid.

6.2 Commissioning

In the beginning of this chapter, methods for commissioning and putting into operation of the transverse feedback system will be described and discussed. The measurements with beam were carried out in two different beam periods and on the two different accelerators:

Measurements at the ESR were done in the summer of 2000. The goal of these measurements was to collect first experience with the beam. The results were important for the first test and for the verification of the theoretical calculated coupling impedance. The new different measurement methods were verified. The results from these measurements were used for the possible correction on the measurement device and on the TFS.

Measurements at the SIS were done in the summer of 2001. The goal of these measurements was to verify the theoretically calculated TFS parameters, to put the transverse feedback system into operation, and to do the first measurements with the TFS and to check the efficiency of the transverse feedback system.

6.2.1 Measurement methods

The natural method is to have the “natural” coherent instabilities. But if there is no heavy impedance source, which can cause strong coherent instabilities or we can not achieve sufficient intensities, we artificially excited coherent betatron oscillations by other alternate methods.

In the following the alternate methods for generation of the “artificial” coherent instabilities will be described. The goal of this part is to give the comparison of the used measurement methods.

The following methods will be discussed and the measurement results achieved with these methods will be presented:

The first method uses the “artificial” coherent instabilities produced by the electron cooling system. In our case the electron cooler was used with a (electron) current of 750mA . This method is only useful for a first commissioning, because one has to separate the effect of the electron cooling system and the TFS. Coherent instabilities produced by an electron cooler are accidental. This method was used in the ESR.

The second method is based on the “artificial” kicking of the beam by an exciter. For this purpose the appropriate power should be used for the kicking of the beam. In this case the synchronisation of the kick and measuring instrument is very important. This method was used in the ESR as well as in the SIS.

The third method is based on the “knock-out” extraction. This method is based on dynamical Q - value measurement. The main principle is the noise excitation. We can use it during all accelerator modes (in acceleration mode, on the flat top, with bunched beam and coasting beam). For the first tests with the transverse feedback system the noise excitation on the flat-top was used. This method was used in the SIS.

6.2.2 ESR measurements with beam

The measurements described in the following were done in the Experimental Storage Ring (ESR). Since the ESR uses the identical position pickups (pickup construction is the same) and the “old” transverse feedback system (for coasting beam and for specific range of the kinetic energy only) is already installed in the ring, the condition for measurements are comparable with the environment in the SIS. Therefore results from measurement with beam can be compared with measurements in the SIS.

The following reasons imply to carry out the first measurements in the ESR:

- In the summer of 2000 the exciter required for the TFS was not yet installed at the SIS.
- Due to safety reasons during a medical beam time it was not possible to use the SIS for machine measurements.
- At the SIS was no transverse feedback system installed. For the first measurements the “old” transverse feedback system at the ESR was used.
- Possible usage of the new transverse feedback system for the ESR too.

The alternate methods for generation of the “artificial” coherent instabilities had to be used. The two different methods for generation of the “artificial” coherent instabilities were investigated in the ESR: “artificial” coherent instabilities excited by electron cooling and the “artificial” kicking of the beam by means of the kicker. Measurements with *coasting beam* were done with a $^{12}\text{C}^{6+}$ beam at a kinetic energy of 260 MeV/u ($\beta = 0.622$). During the test the kinetic energy was changed in range from the 250 MeV/u to 300 MeV/u . To achieve the desired higher intensities stacking together with electron cooling had to be used. Beam currents up to $\approx 5.5\text{ mA}$ were accumulated.

The “artificial” coherent instabilities produced by the electron cooling system.

The coasting beam was cooled up to a density level where “artificial” coherent instabilities could be observed. At this moment the old active feedback system was switched on manually. The disadvantage of this method is that one has to separate the effect of the electron cooling system and of the TFS. The second disadvantage is the reproducibility of the “artificial” coherent instabilities. The coherent instabilities produced by electron cooling system are accidental.

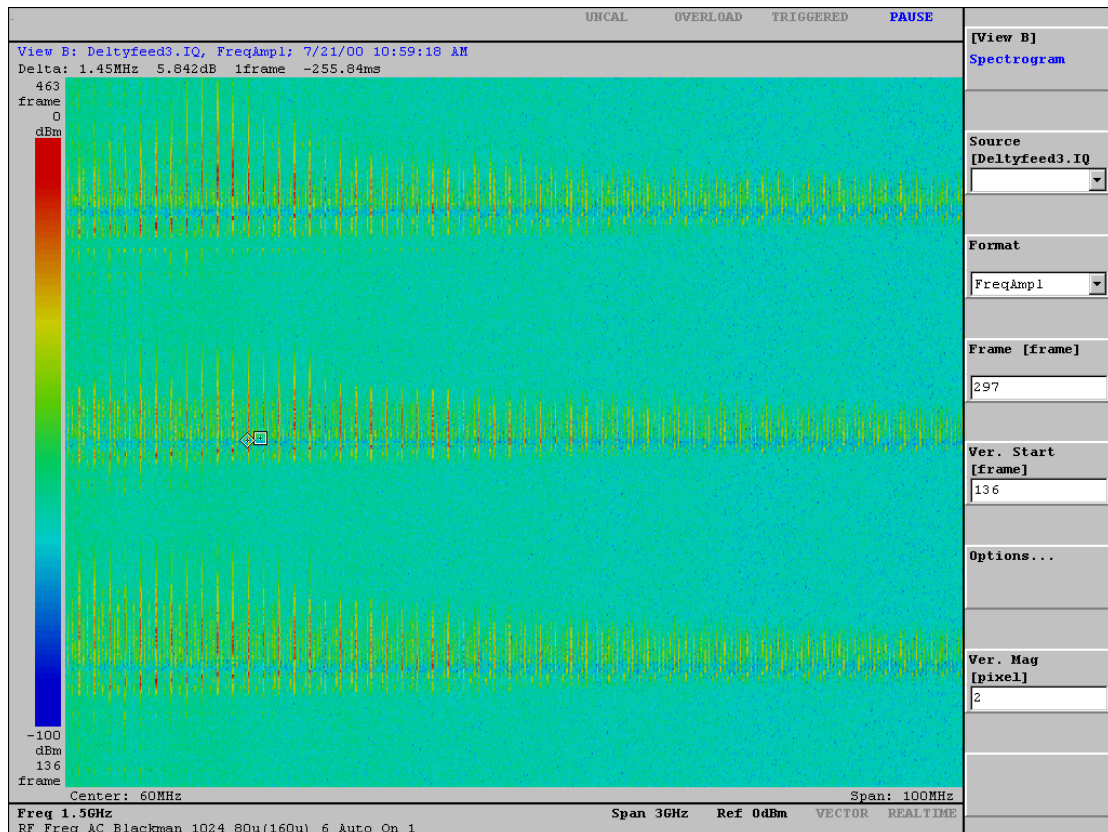


Figure 6.5: The “artificial” coherent instabilities were produced by electron cooler and the TFS was switched on. The measurement with the TFS was reproduced three times. (the TFS was switched on and off 3 times.) (Measurement was done in the ESR.)

The measurements results with coasting beam are shown in figure 6.5. The feedback system was switched on and off 3 times. In figure 6.5 the difference signal from Schottky pickups is shown. The reason is that the difference signals from position pickups are such small signals that after subtraction it is not possible to see the difference signal. The measured frequency range is up to 100 MHz. The “artificial” coherent instabilities caused by the electron cooler are very intensive up to 60 MHz. The measured damping times can be only estimated from the plot because synchronisation of the feedback system and generation of the instabilities was very hard. The feedback system could be controlled only manual. The estimated damping times are approximately 200 ms. The “artificial” coherent instabilities produced by the electron cooling system can be used for the first tests but such a kind of coherent instabilities can not be used for exact evaluation of the

damping constant. Optimal setting depends on the gain of the preamplifier for pick-ups. If pick-up preamplifiers are saturated the signals from pick-ups are not usable.

The ‘artificial’ kicking of the beam by an exciter installed in a ring.

The method is very simple: a coherent horizontal or vertical oscillation is excited by a single kick and the centre-of-charge position of the beam in the coasting beam is observed approximately 200 ms that corresponds over 40000 turns at injection energy. The damping rate observed in the experiment is the sum of the damping of the TFS and the natural damping (Landau damping). To extract the damping rate of the TFS alone, we need to subtract the effect of the natural damping from that of the experimental data. The rate of the natural damping is easily measured by the experiment with the TFS off.

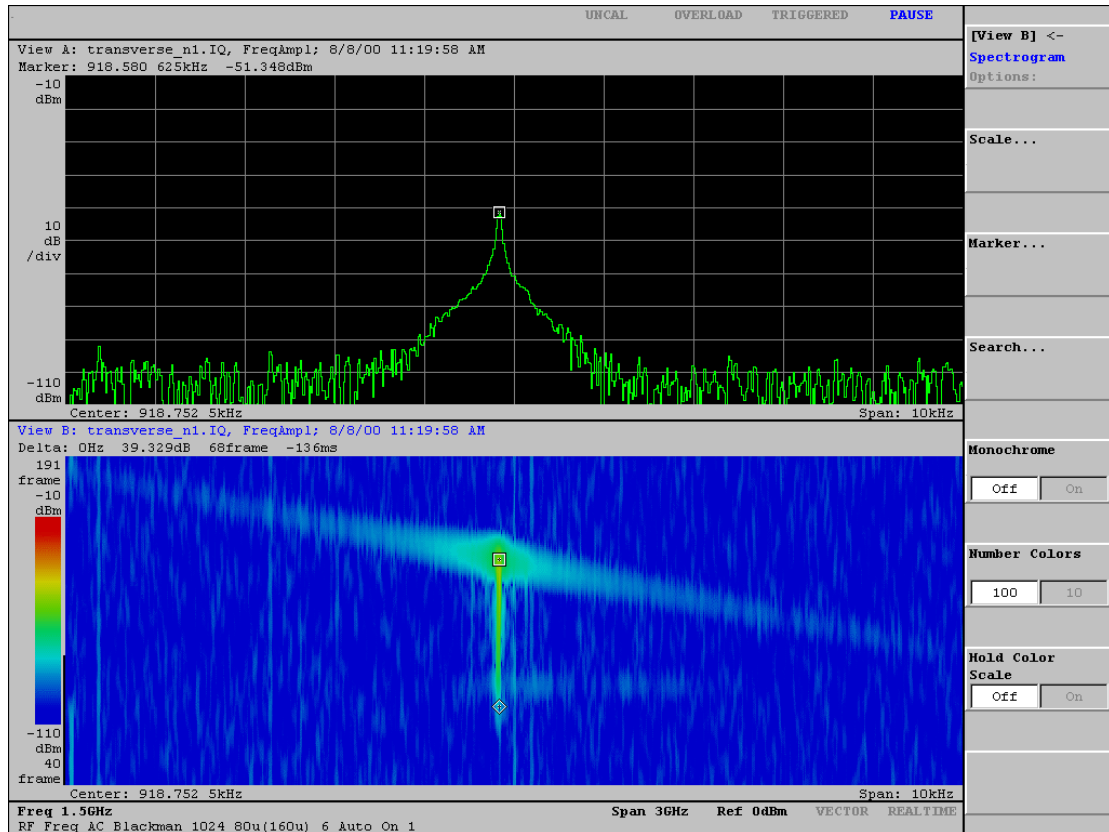


Figure 6.6: Methods for pre-commissioning of the TFS. The measured natural damping time is approximately 136 ms. (Measurement were done in the SIS.)

This method could not be applied in the ESR because the kick power (with the lowest voltage at kicker) was too strong and the beam was kicked out of the acceptance regularly.

The possibility to use this method in the SIS was proved. These measurements were done with a $^{197}\text{Au}^{65+}$ beam at the injection energy level of 11.4 MeV/u. The setting of the machine in the SIS was as following:

$$E_{\text{kin}} = 11.5 \text{ MeV/u} \quad f = 850.030 \text{ kHz} \quad \beta = 0.158$$

$$Q_x = 4.29 \quad Q_y = 3.24 .$$

In figure 6.6 two plots are shown from SIS. The first plot (upper) represents a spectrum at one time step. The signal of the upper sideband (fast wave) is shown for the 4th harmonics with the frequency span 10 kHz. The second plot (lower) shows the three dimensional figure of the upper sideband at frequency 918,752 kHz. The red color represents the highest intensity or signal and the blue color represents the lowest intensities. The difference between both cursors corresponds to the natural damping time. In this case the measured natural damping time is approximately 136 ms.

6.2.3 SIS measurements with beam

The series of new measurements were taken in the summer of 2001. All these measurements were done with the new transverse feedback system installed in the SIS. The goal of measurements carried out in the SIS was to check the operation of the digital signal processing with the beam and to collect experiences with the new transverse feedback system which works automatically for all accelerator modes.

Measurement conditions

At first the measurement conditions are described. The coasting $^{197}\text{Au}^{65+}$ beam at the extraction energy of 350 MeV/u was used for the all measurements discussed below. In the SIS was tested.

An example of the transverse vertical coherent sidebands for the 20th harmonics of a $^{197}\text{Au}^{65+}$ beam at the extraction energy of 350 MeV/u is shown in figure 6.7. The setting of the machine in the SIS was as following:

$$E_{\text{kin}} = 350 \text{ MeV/u} \quad f = 3800.31 \text{ kHz} \quad \beta = 0.68$$

$$Q_x = 4.30 \quad Q_y = 3.29 .$$

The fractional q_x - value was set to 0.30 and the measured fractional q_x - value was 0.32. This difference is due to an error between setting devices in the accelerator and controlling software. The frequencies correspond to the 290.1 kHz and 306.2 kHz, respectively. The measured centre frequency is 18.999545 MHz and the theoretical calculated value of centre frequency is 19.00155 MHz.

An example of the measured spectrum of the signal generator is shown in the figure 6.8. The described measurement were carried out on the flat top. The following reasons lead to measure on the flat-top:

- We had no "natural" coherent instabilities.
- In order to put the transverse feedback system into the operation we need reproducible method for instabilities for a longer time (\approx seconds).
- The effect of the TFS can be separated from other effects.

The "artificial" coherent instabilities produced by the "knock-out" method.

The description of the measurement method is based on the figure 6.9. Two plots are presented:

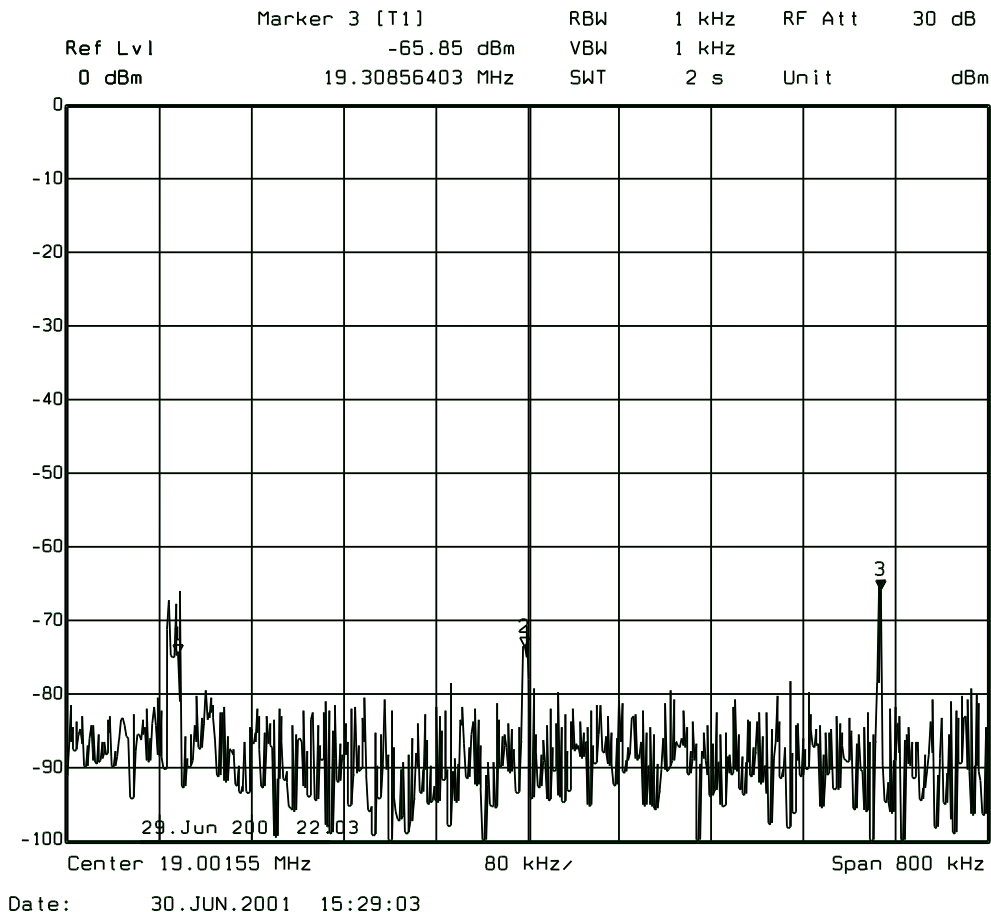


Figure 6.7: Lower (1) and upper (3) betatron coherent sidebands in the horizontal direction for the 20th harmonics of a $^{197}\text{Au}^{65+}$ beam at the extraction energy of 350 MeV/u. In the center $f=19,00155$ MHz (2) is the longitudinal signal.

- **The relative amplitude of the noise generation** represents our coherent instabilities. The noise was only generated on the flat top and was triggered with the beginning of the flat top phase. The noise was generated within 2 seconds.
- **The relative amplitude of the current transformer** corresponds to the beam current in the ring. The measured characteristic is divided into four different phases (A, B, C, and D) which are described below. The most important is the C phase.

At the beginning of the phase A particles are accumulated in the ring at the $\beta = 0.15$ (phase A - accumulation phase). Then the beam is accelerated from $\beta = 0.15$ to $\beta = 0.68$ (phase B - acceleration phase). After the acceleration phase the beam is circulated in the SIS for a number of seconds (phase C - flat-top phase with the slow extraction). As it can be seen from the figure 6.9 at the begin of the flat-top phase the noise generation is triggered and started automatically. The beam is excited for a number of seconds continuously. The so-called slow extraction is started. To avoid the beam extraction (beam losses) the TFS should be switched on. The different decreasing slopes correspond to different input parameters adjusted for the TFS. The four different cases in depending on the input parameters were measured and are discussed in the following: the TFS is switched on or off, the noise generation is switched on or off, and one or both pickups for

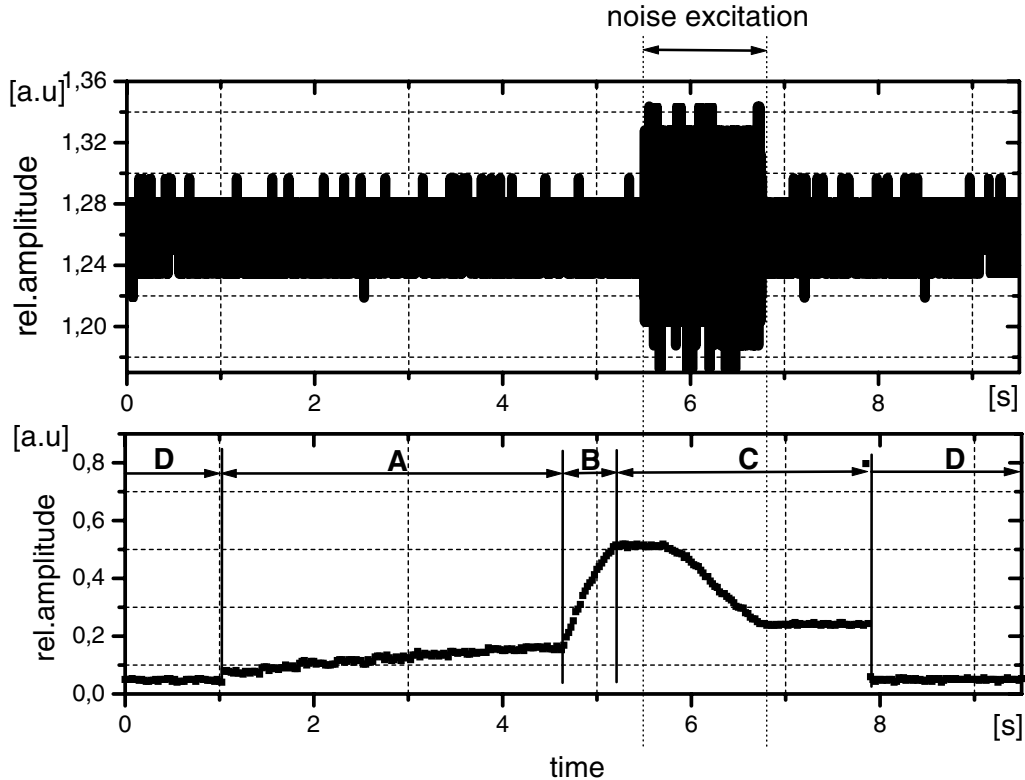


Figure 6.9: Two characteristics represent the relative amplitudes of the noise generation (KNOCK-OUT) and of the current transformer. The four phases specify: A - accumulation phase, B - acceleration phase, C - flat-top phase with the slow extraction and D - start and stop phase of the accelerator cycle.

beam is stable and without external excitation (no coherent instabilities) and the transverse feedback system is switched on then no influence on the beam caused by TFS alone was (as is shown in the figure 6.10 plot TFS_4) observed.

TFS_2: Input measurement conditions:

$$\text{TFS}=\text{on} \quad (\text{S04DX5H}=-0.4, \text{S05DX5H}=0.7) \quad \text{knock-out}=\text{on} .$$

The plot TFS_2 represents the situation when both pick-ups are used. The beam losses were about 40% smaller in comparison to the situation with TFS switched off (plot TFS_4).

TFS_3: Input measurement conditions:

$$\text{TFS}=\text{on} \quad (\text{S04DX5H}=-0.4, \text{S05DX5H}=\text{off}) \quad \text{knock-out}=\text{on} .$$

The plot TFS_3 represents the situation with the TFS switched on but the signal from one pick-up is only used. The improvement on the beam stability of about 27% was measured.

TFS_4: Input measurement conditions:

$$\text{TFS}=\text{off} \quad (\text{S04DX5H}=\text{off}, \text{S05DX5H}=\text{off}) \quad \text{knock-out}=\text{on} .$$

plot	TFS [on/off]	S04DX5H [on/off]	S05DX5H [on/off]	knock-out [on/off]	beam losses [%]
TFS_1	on	on	on	off	0
TFS_2	on	-0.4	0.7	on	62
TFS_3	on	-0.4	off	on	73
TFS_4	off	off	off	on	100

Table 6.1: The evaluation of the TFS efficiency with the beam. In the column “plot” the TFS_1, TFS_2, TFS_3, and TFS_4 corresponds to plots in the figure 6.10.

In the plot TFS_4 the standard beam behaviour in the ring with the feedback switched off is shown. The TFS is switched off and after certain time is the beam kicked off. This plot represents the reference value.

The multiplication coefficients can be changed in the range from -2 to 2. The correct and optimal values for the coefficients are calculated from the betatron functions. The system gain can be adjusted at three different positions: amplifiers for pick-ups, system amplifier (behind the digital part of the TFS) and power amplifier. The system gain for all measurements was set to a constant value.

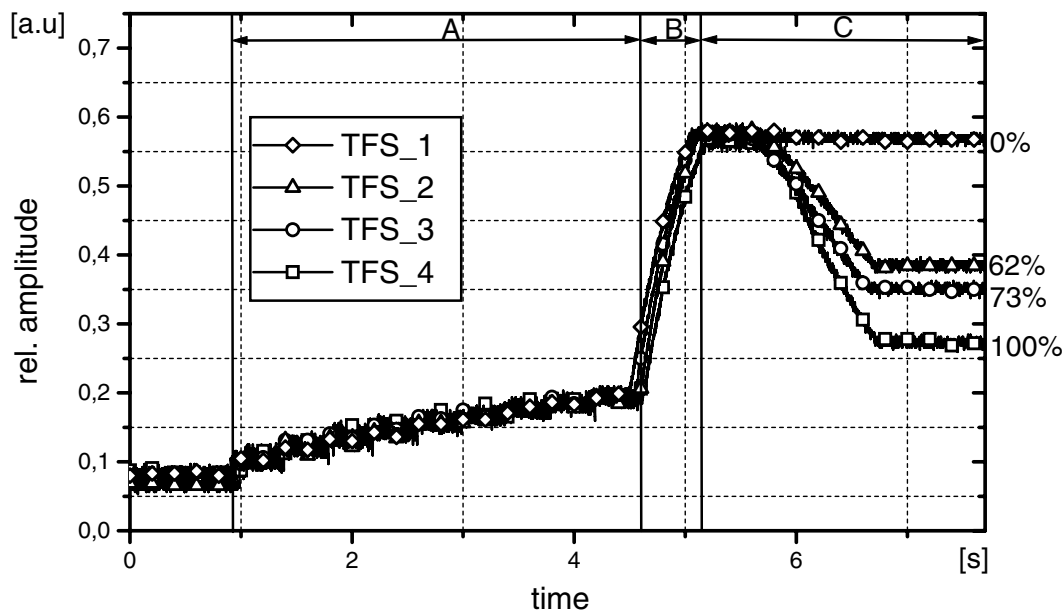


Figure 6.10: Results from measurement in the horizontal direction in the SIS. The different input conditions are listed in the table 6.1.

The TFS was successfully tested under different input conditions. The summary for measured characteristics with corresponding input conditions is listed in the table 6.1. In order to increase the TFS efficiency the TFS in both directions (horizontal and vertical) should be used (coupling between horizontal and vertical plane). Experiences from the measurements have shown that the correct coefficient sign and coefficient value is very important. If the coefficient sign is not correct the TFS can not damp the instabilities but can excite the coherent instabilities.

6.3 Conclusions

From the measured spectrums the conclusion can be drawn that the Schottky pickups are wide band systems and that the position pickups are very sensitive in the low frequency range where the instabilities occur.

To put the transverse feedback system into operation requires periodical "coherent instabilities". During the measurements with beam, three alternate methods for "artificial" coherent instabilities were presented: "artificial" coherent instabilities produced by electron cooling system, "artificial" coherent oscillations by kicking the beam with the kicker, and "artificial" coherent instabilities produced by "knock-out" method. The onset of instabilities for the first two methods is more a stochastic process. Therefore the transverse feedback system should be switched on manually. For this reason the exact evaluation of damping times could not be performed.

For the mentioned reasons the best way to test the efficiency of the transverse feedback system is to use the "artificial" coherent instabilities produced by the "knock-out" method. For the digital feedback system the "knock-out" method was successfully tested. A very important point should be mentioned at this place: reproducibility. The best results were achieved with the vector summation. As we can see from measurements an increase of the beam intensity by more than 40 % was achieved.

The functionality was checked in manual mode as well as in the automatic mode. In the manual mode the four input parameters can be adjusted: coefficients for the vector summation, the system gain in the feedback loop and the revolution time (delay time). In the automatic mode we can choose which parameters will be set up and calculated automatically, and which parameters will be set up manually.

From the table 6.1 we can see that the TFS is working with one pick-up but the TFS efficiency can be higher with the vector summation. More tests with the TFS especially with different feedback loop gains, coefficients etc. are planned to be done. The disadvantage of this method is that during measurements it is required to have a constant level of the beam intensity. If this condition is kept the TFS system can be tested under different conditions.

Chapter 7

Conclusions and outlook

The work was motivated by the need to control coherent transverse instabilities in a broad velocity range and to find new concepts and methods for improving the efficiency a broadband TFS. All transverse feedback systems were constructed exact only for one accelerator. The main reason is that the most parts of transverse feedback systems are distributed (long cable delays) and were designed exact only for one system. Transverse feedback systems already in use at different accelerators were not able to cover all working accelerator modes (coasting beam, bunched beam, acceleration mode) and the adaptation for different accelerators was not simple. The presented transverse feedback system solves all these problems. The constructed system is compact, highly adaptable and customisable, and, in principle, can be used for all accelerators. The change of some constants in the system make possible to use it for different accelerators. The digital system has unlimited possibilities and can be used for all acceleration operation modes (flat-top, during acceleration, coasting beam, bunched beam, the variable delay is configurable). The advantage of the system is that the digital system allows to work in the manual mode as well as in the automatic mode. The manual mode is used from the beginning for the basic adjustments and for putting the transverse feedback system into operation.

Within this thesis, the increasing of the beam intensity limit by means of the automatic feedback system operating in a large velocity range of ions was investigated and the practical realisation was presented. A systematic theoretical analysis of coherent instabilities in the SIS of GSI as well as an analysis of feedback system parameters was performed. A digital signal processing part, which is a crucial component of the SIS transverse feedback system, was designed and constructed. The practical tests show that the digital signal processing is a very promising method and can not only be used for feedback operation but also for feedback system diagnosis.

Theoretical consideration

The change of betatron functions at pick-up and exciter positions during the acceleration process in the SIS was calculated. From triplet focusing mode (at injection energy level) to doublet focusing mode (at extraction energy level) the betatron function value is changed by more than a of two factor.

The transverse coupling impedance has been analysed in detail. As a main contributions to the real part of the coupling impedance, the resistive wall and kicker impedances were identified. These are the most important impedance values in the low frequency range where the Landau damping is insufficient. The kicker impedance with magnitude

of approximately 800 k Ω /m at the frequency of 14 MHz was measured as the most dangerous [21]. The broadband impedance is dominant for higher frequencies. The most important contribution to the imaginary part of the transverse coupling impedance is the space-charge impedance which can reach values of 1.1 G Ω /m.

The equation for the feedback impedance – including transfer functions of electrostatic pick-up and strip-line exciter – was derived. The effect of the exciter length on TFS efficiency in the higher frequency range as well as time difference between particle-flight time and electrical time were analysed. Taking into account the above mentioned analysis, a new exciter with a length of 15 cm was designed and installed in the ring.

Because the heavy ion synchrotron SIS was designed for operation at the space charge limit, a precise analysis for a U_{238}^{72+} beam with $3 \cdot 10^{10}$ particles (assuming an elliptic beam distribution) was performed. In order to cover all energies and accelerator working modes, the stability diagrams and rise times for other species were also considered. Two cases for transverse stability were studied in detail: a coasting beam at injection energy ($\beta = 0.158$) and after an acceleration process ($\beta = 0.58$). The estimated rise time at frequencies, where the Landau damping is effective, is approximately 0.5 s and, therefore, are not as dangerous as coherent instabilities coming from the kicker with an estimated rise time of 15 ms. Such coherent instabilities might become a problem after 100 ms and especially for 14 MHz where the maximum of the transverse coupling impedance is supposed to be. From analysis performed, the entire frequency range up to 40 MHz can be dangerous and should be controlled by a transverse feedback system. Because the instability rise time is smaller than the time of the acceleration process the TFS must work during the acceleration process too. Thus, a programmable variable delay with parameters listed in table 4.3 is required.

An overview of feedback systems together with a discussion and comparison of digital and analogue systems was given. Most of the listed analogue possibilities are not programmable or can be only slightly modified during operation. However this is insufficient for modern automatic transverse feedback systems. The possibilities for variable delays were investigated and compared in detail. Concerning the design of a new TFS, we conclude that the main problems are to realise broadband non-dispersive variable delay times in the range up to 10 μ s (for correction in the second turn) and to allow mathematical operations in real time. The different phase-advance adjusting methods were discussed and compared, too. The complete analysis of these methods - vector summation method - with the possibility to change the TFS parameters and to calculate the required signal for the exciter online, without interruption of the output signal, was presented.

Simulations

In the frame of this work the beam with the feedback system for various boundary conditions was simulated. A wide variety of cases was investigated to document the effect of multiplication error (phase advance error), quantization noise, pick-up noise (resolution), exciter length, exciter transfer function and system gain. The comparison of different working methods (proportional and constant kick) under different conditions were also presented. The results obtained from these simulations show which parameters are important for the design of a new TFS. We demonstrated, for instance, that:

- damping time for 40° phase advance between pick-up and exciter is by factor 2 bigger than for 90°.

- reciprocal value of the horizontal damping time is linearly dependent on the system gain.
- for a certain exciter length and time difference between particle flight time and electric transit delay time, an upper limit value of the frequency exists where the feedback system does not work.
- a constant damping scheme provides a linear damping of the amplitude and additionally, for the same peak power it is faster than the conventional proportional damping scheme which produces an exponential damping in time.

Concerning the design of a digital signal processing system we found the following conclusions:

1. A 12 bit/100 MHz system with variable parameters is required for the signal processing because of the dynamic range, system resolution and analogue frequency range up to 40 MHz to be processed.
2. The tasks are divided between PLD and DSP, i.e. PLD is used as DSP coprocessor because the PLD can handle repetitive functions with extremely high performance and the DSP processor can perform remaining functions.
3. Parameter independent phase characteristic in the whole frequency range is required. The transfer function of the TFS should not depend on adjusted value of programmable variable delay.
4. Calculation in real time of the correct signal for the exciter is required. A new signal is received each 10 ns and in the same time the calculated signal has to be used at the exciter. Thus, a maximum peak data processing rate of 800 Mbytes/s is required.
5. The digital signal processing method offers the possibility to use both proportional and constant damping scheme.

Design

These facts were the motivation for a new development of the digital signal processing part, the design and realisation of which was divided into the two parts:

main card with PLD - it processes both pick-up signals and calculates the signal for the exciter.

control card with DSP - it acts as a watch-dog for the main card. Because both pick-up signals are available on each clock pulse the processed signals from the *control card* have to be sent into the *main card* without disturbing the data processing from pick-ups.

By means of new signal processing methods the switching times for the variable delay and notch filter were optimised. That means that the switching time does not depend on the value of the variable delay time.

Because delay-step values of the digital signal processing system are given by the reciprocal value of the clock frequency, novel methods (digital and analogue) for increasing of the delay-step value were studied and a practical solution was presented. The digital

method with a resolution of 1 ns was simulated. For practical realisation, the analogue version with switchable delay lines was presented.

A new phase adjusting method for vector summation with auto-changing coefficients was discussed. For this purpose, four different ramps are generated during the whole acceleration process: revolution time, multiplication coefficients and total gain. This allows to adjust the feedback system for all working modes optimally: coasting beam, bunched beam and during the acceleration process.

The detection method using two pick-up signals requires two different delays: short delay between both pick-ups S04DX5H and S05DX5H ($60 \text{ ns} \div 400 \text{ ns}$) and long delay between pick-up S05DX5H and exciter S04TFH ($700 \text{ ns} \div 9.64 \mu\text{s}$). Both short and long delays were integrated on a single 30KE chip by means of dual port memory.

The simulations have shown that by using the optimisation and pipelining methods that the maximum system clock frequency can be increased by factor of 3. For the whole TFS design the maximum simulated clock frequency 131.5 MHz with adjusted output latency for multiplication and summation of 3 clock cycles was achieved.

The integrated solution for the new feedback system was presented and a method for online digital signal processing has been developed and put into operation. According to the accelerator working mode the TFS can work in automatic or manual mode of operation. In manual mode (by means of program NODAL) values for revolution time, multiplication coefficients as well as total gain can be entered.

Measurements

The realised 12bit/100 MHz variable digital signal processing working in real time shows results which are in a very good agreement with the theoretically calculated parameters. The phase error within the entire frequency range is less than $\pm 4^\circ$. The measured available precision of the programmable variable delay for the TFS is to 146 ps. The RMS value (the delay step value was $n = 100 \text{ ns}$) of the deviation from the nominal value was found to be 201.4 ps. Correction and optimisation methods for improving parameters like differential and integral nonlinearity were presented and applied. First measurements with the variable notch filter showed the results expected. A notch depth up to 30 dB in the frequency range from 2 MHz to 15 MHz was measured.

For feedback system optimisation and parameter calculations the SIS and ESR measurements were performed. To demonstrate the quality of the digital signal processing part the first test and commissioning with the automatic transverse feedback system were carried out in the ESR.

To put the transverse feedback system into operation requires periodical "coherent instabilities". During the measurements with beam, three alternate methods for "artificial" coherent instabilities were presented: "artificial" coherent instabilities produced by using the electron cooling system to achieve beam phase densities to induce instabilities, "artificial" coherent oscillations by kicking the beam with the kicker, and "artificial" coherent instabilities produced by "knock-out" method. The first two methods are more stochastic processes and the transverse feedback system should be switched on manually. For this reason the exact evaluation of damping times could not be performed.

For the mentioned reasons the best way how to test the efficiency of the transverse feedback system is to use the "artificial" coherent instabilities produced by the 'knock-out' method. This method was used as a compromise among others methods. For the digital feedback system the "knock-out" method was successfully tested. The very important

point should be mentioned at this place: reproducibility. The best results were achieved with the vector summation. At the beginning we supposed that an increase of the beam intensity by factor 2 could be possible in the SIS ring with the transverse feedback system. As we can see from measurements an increase (improvement) of the beam intensity more than 40 % was achieved.

Many extensions of the present work are possible as future challenges. Within this work the required intensities for “natural” coherent instabilities could not be achieved in the SIS at the GSI. In addition, only measurements with a coasting beam could be performed. The complete and exact analysis of each parameter ($\Delta\tau, Q, noise, \dots$) should be examined within the entire frequency range.

Concerning bunched beams, work has to be done to study the behaviour of both the notch filter and the BOSS (Beam Offset Signal Suppressor). More measurements in both directions (horizontal and vertical) is required to evaluate the behaviour of the notch filter (especially the phase characteristic, see chapter 5.2.2) in interaction with beam.

Furthermore, the different damping methods (see chapter 4.1.2 and chapter 4.5) should be subjected further investigation. Results from these measurements can tend to better understanding of the beam and TFS interaction.

Appendix A

Symbols and constants

A	mass number or amplitude
A_D	effective noise value due to quantization
a	is 16/3 for parabolic distribution function and 64/15 for quartic distribution function
b	radius of vacuum chamber
b_{par}	feedback factor $0.0 \leq b_{par} \leq 1.0$
$\vec{B}(\vec{r}, \omega, s)$	magnetic field
B_D	noise power added to a signal due to quantization
c	speed of light (vacuum)
C_{PU}	pickup capacity
$d(t)$	time-dependent dipole moment
d_k	half height and width of kicker gap
E_{kin}	kinetic energy
$\vec{E}(\vec{r}, \omega, s)$	electric field
E_0/e	proton rest mass in volts (938 MV)
e	elementary charge (1.6022×10^{-19} C)
f	frequency
f_0	revolution frequency
f_s	sampling frequency or synchrotron frequency
f_β	betatron frequency
f_{nmp}	frequencies of coherent transverse modes
f_{min}	lower frequency limit for transverse feedback system
F_W	driving term for betatron oscillations
$\tilde{F}^W(\omega)$	Fourier transformation of F_W
$\tilde{F}^{FB}(\omega_1)$	Fourier transformation of feedback term
g	geometrical factor
G	total gain in feedback loop
$G_{absolute}$	absolute gain
h	harmonic number
h_K	width of exciter gap
h_{PU}	width of pickup gap
I, I_B	ion beam current
I_C	charging current
K_\perp	figure of merit for transverse exciter
$k(s)$	periodic function

L	synchrotron period length
l_K	exciter (kicker) length
l_{PU}	pickup length
M	number of bunches
m	mode number; describes the phase relation between particles within a bunch
m_0	mass of a particle
N	number of stored ions
n	mode number; the coupled bunch mode; or number of bits
p	mode number; describes periodicity in transverse phase space
p_{\perp}	transverse momentum
q	fractional part of tune or charge state (q/A)
q_{charge}	image charge on the plate
q_x	fractional part of the horizontal tune
q_y	fractional part of the vertical tune
q_D	quantization level or resolution of the ADC
Q	tune
Q_x	horizontal tune
Q_y	vertical tune
Q_{cav}	quality factor of resonator
R	synchrotron circumference
R_{IN}	input impedance of preamplifier
R_s	shunt resistance of resonator
r_{beam}	beam radius
s	longitudinal coordinate - coordinate along to design orbit
t	time
t_0	intrinsic delay
$T_{revolution\ time}$	revolution time
$u(s)$	general coordinate for horizontal or vertical direction
\vec{v}	particle velocity
v_B	particle velocity βc
V	output voltage at pickup
V_P	output voltage at pickup
V_K	input voltage at exciter
V_L	voltage at stripline pairs
x	horizontal distance coordinate
x'	angel between particle and design orbit in the x - s -plane
$x_0(t)$	input signal depending on time
\hat{x}	maximum amplitude of transverse oscillation assumed to be one-dimensional
x_i	transverse position error of i -th bunch
x_A	initial amplitude in vertical direction
$X_i(\omega)$	Fourier transformation of x_i
y	vertical distance coordinate
y'	angel between particle and design orbit in the y - s -plane
$y(t)$	output signal depending on time
y_A	initial amplitude in horizontal direction

y_{PU}	coherent oscillation amplitude at pickup position
y_{K}	coherent oscillation amplitude at exciter position
Z	ion charge state
$Z_{\perp}(\bar{r}, \omega)$	coupling impedance
Z_{\perp}	transverse coupling impedance (x or y direction)
Z_{\perp}^{SC}	space charge impedance
Z_{\perp}^{RW}	resistive wall impedance
Z_{\perp}^{BB}	broadband impedance
Z_{\perp}^{K}	kicker impedance
Z_{\perp}^{EC}	electron cooling impedance
Z_{\perp}^{FB}	transverse feedback impedance
Z_0	the impedance of free space
Z_C	characteristic impedance
Z_L	impedance of stripline pairs
Z_k	impedance of external network
$W_{\perp}(\bar{r}, s)$	wake function
w_{K}	height of exciter gap
w_{PU}	height of pickup gap
α	alpha function
α_{att}	attenuation function
$\alpha_{x,y}$	alpha function (horizontal, vertical)
$\alpha_{\text{PU},x}$	alpha function at the pickup (PU) position for the x direction
$\alpha_{\text{PU},y}$	alpha function at the pickup (PU) position for the y direction
$\alpha_{\text{K},x}$	alpha function at the exciter (K) position for the x direction
$\alpha_{\text{K},y}$	alpha function at the exciter (K) position for the y direction
β	relativistic velocity factor v/c or betatron function
β_{att}	attenuation function
$\beta_{x,y}(s)$	betatron function (horizontal, vertical)
$\beta_{\text{PU},x}$	betatron function at the pickup (PU) position for the x direction
$\beta_{\text{PU},y}$	betatron function at the pickup (PU) position for the y direction
$\beta_{\text{K},x}$	betatron function at the exciter (K) position for the x direction
$\beta_{\text{K},y}$	betatron function at the exciter (K) position for the y direction
$\bar{\beta}_{x,y}$	average betatron function (horizontal, vertical)
γ	relativistic Lorentz-factor
γ_{T}	relativistic factor at transition energy
δ_i	arbitrary phase constant for particle i
$\delta p/\bar{p}$	width of momentum distribution at half height of maximum
ε	(beam) emittance
ε_x	horizontal emittance
ε_y	vertical emittance
η	off momentum parameter or damping coefficient
$\eta_{\text{t;d}}$	triplet\doublet off momentum parameter
ξ	chromaticity
$\xi_{\text{t;d}}$	triplet\doublet chromaticity
σ	el. conductivity of vacuum chamber wall material
τ	time delay between a generic beam particle and the synchronous particle

$\dot{\tau}$	time derivative of τ
τ_{cool}	cooling time
τ_{p}	particle flight time between pickup and exciter
τ_{e}	electronic delay time
τ_{focusing}	is 1 for triplet and 0 for doublet
τ_{risetime}	coherent instability rise time
τ_{rw}	resistive wall rise time
τ_{k}	kicker rise time
τ_{bb}	broadband rise time
τ_{blowup}	quantization rise time
φ	phase of an oscillation
$\psi(\varphi, \hat{x}, \dots)$	a distribution function for beam
ω	angular frequency
ω_0	angular revolution frequency
ω_r	resonance frequency of resonator
ω_n^{\pm}	transverse signal of a single particle with ω and Q in spectrum with single lines
$\omega_{\perp nc}$	frequency offset
ω_{ξ}	chromaticity frequency
$\Delta\varphi$	phase difference between adjacent bunches
$\Delta\tau$	difference between particle flight time and electronic delay time
$\Delta\mu$	betatron phase advance between pickup and exciter
Δt_{D}	delay step value for digital delay
Δt_{A}	delay step value for analogue delay
Δx	transverse beam displacement
$\delta x'$	kick angle received by ion going through exciter
δ_n	deviation from the ideal value
Δx_{min}	achievable pickup resolution in vertical direction
Δy_{min}	achievable pickup resolution in horizontal direction
Δp_{\perp}	momentum change of particles
Ψ_0	initial phase
$\Psi(s)$	phase function

Appendix B

ALTERA implementation

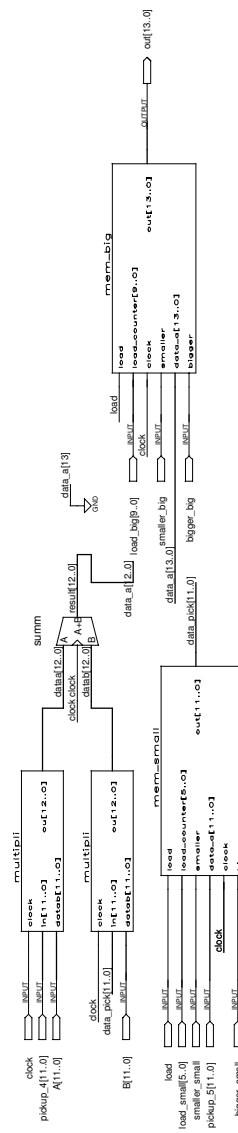


Figure B.1: The entire feedback integrated in the ALTERA chip EPF10K30ETC144-1.

Complete system of the dual port ram - big or small - with automatically running counters

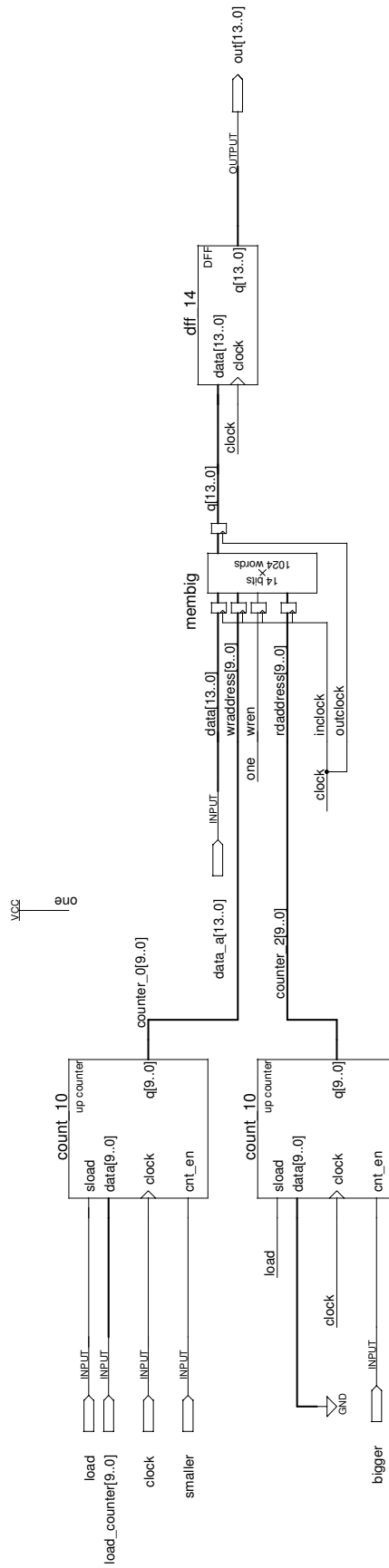


Figure B.2: Memory implementation with automatically running counters in the ALTERA chip EPF10K30ETC144-1.

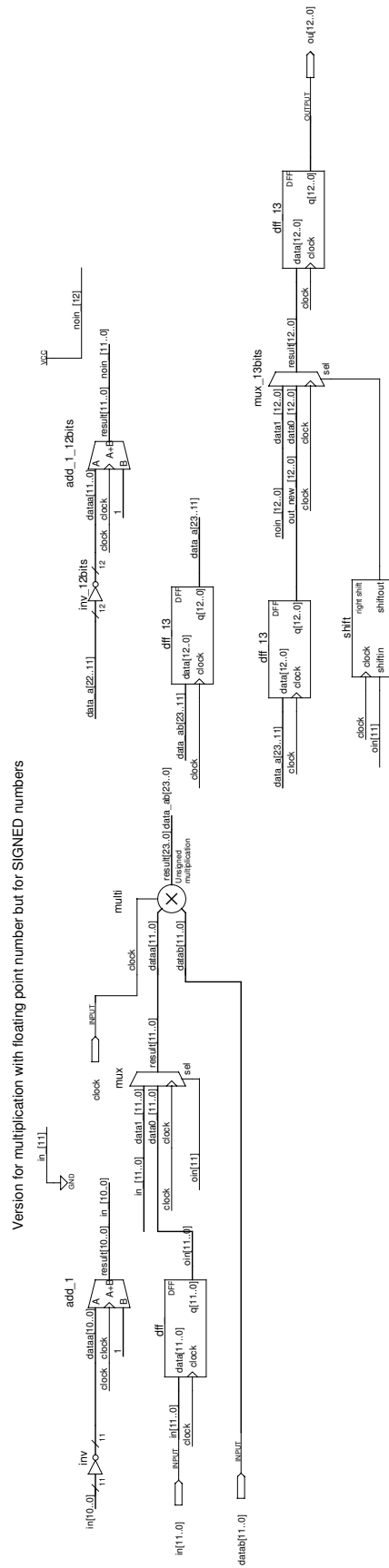


Figure B.3: Implementation of the multiplication with decoding in the ALTERA chip EPF10K30ETC144-1.

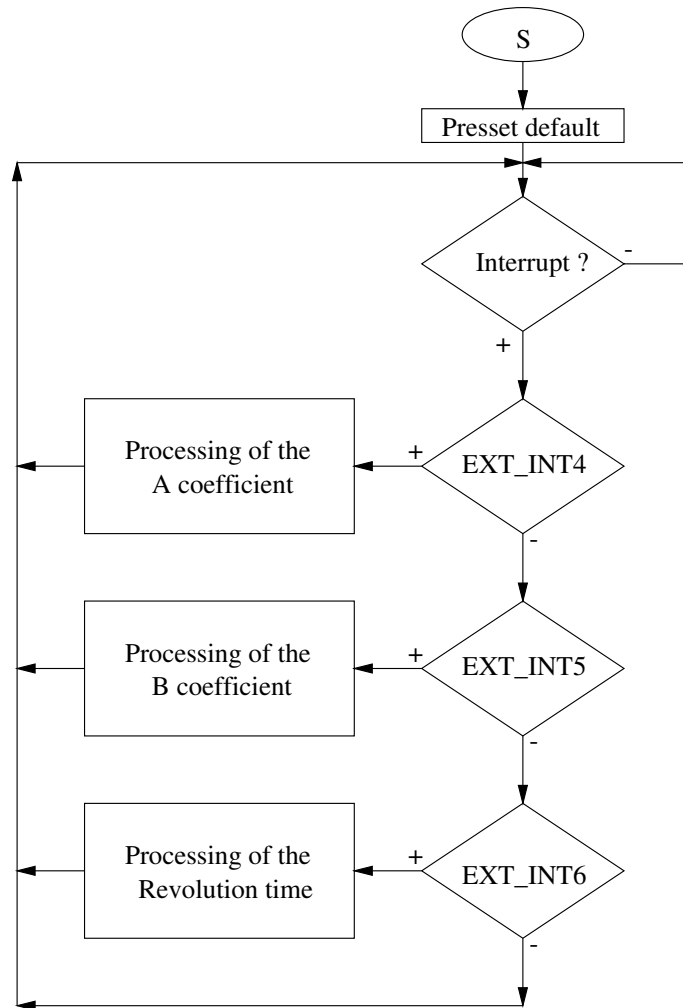


Figure B.4: Data flow diagram for the control card.

Appendix C

Connection diagrams - Main card

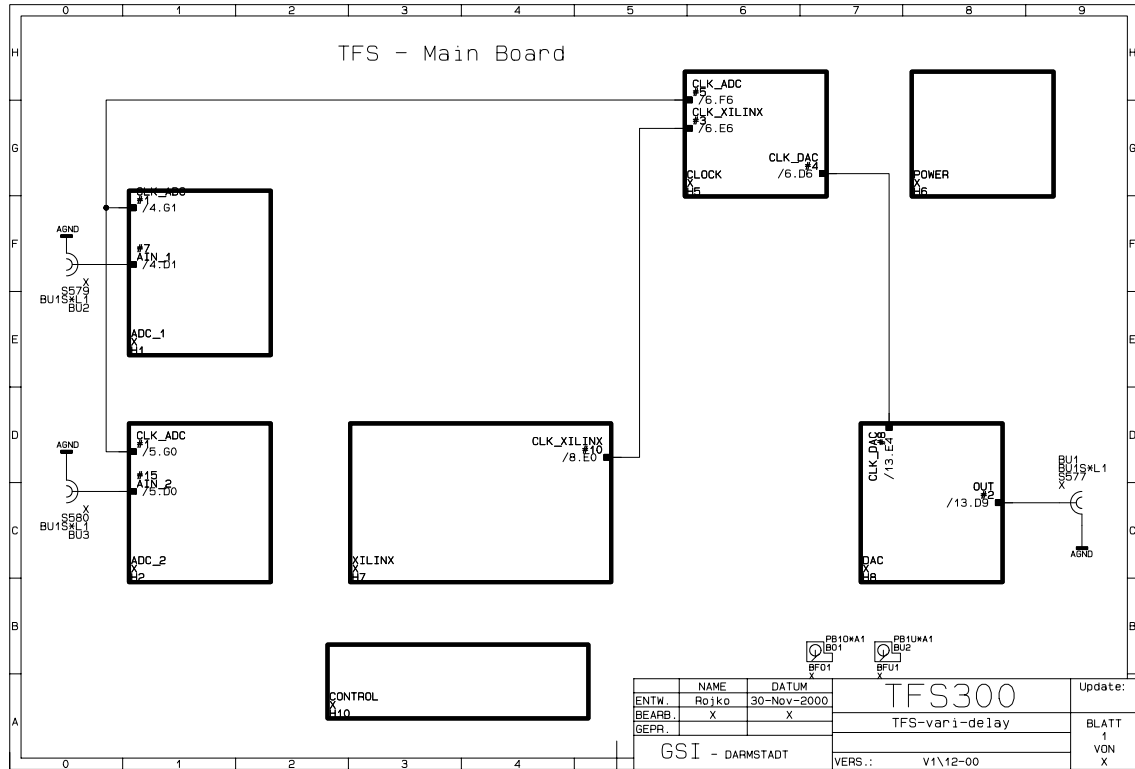


Figure C.1: The principal scheme of the main card presented in modules.

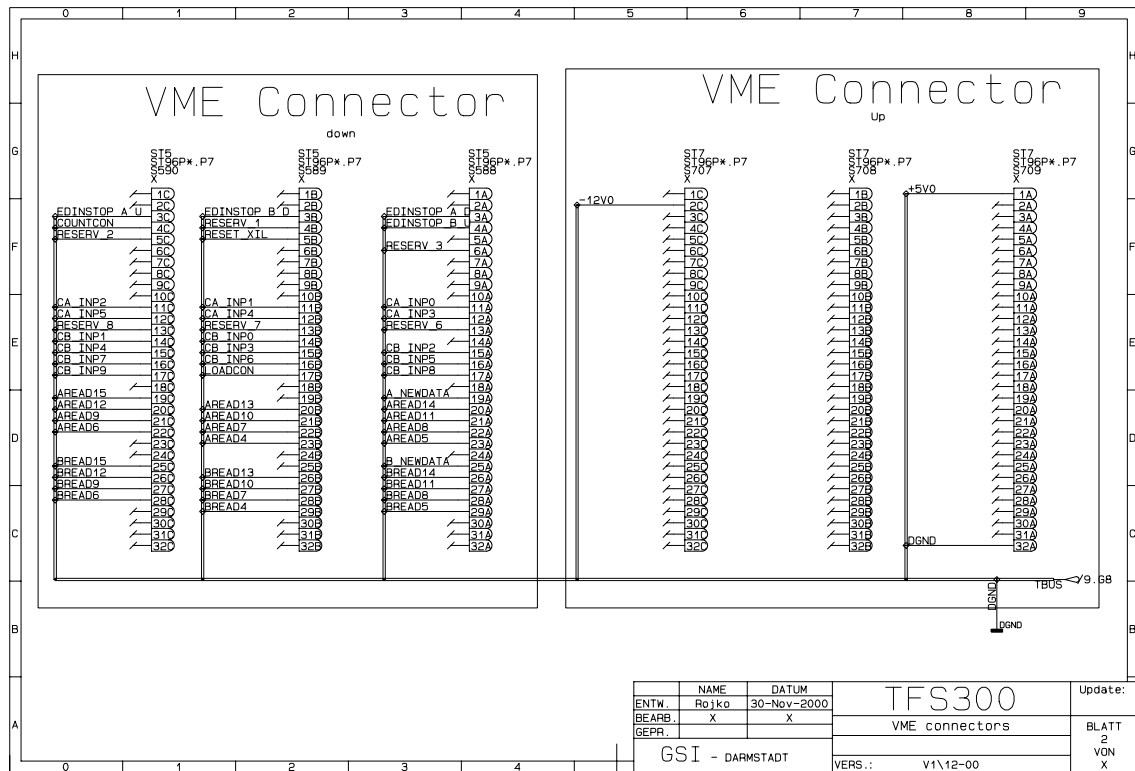


Figure C.2: The VME connectors for connection to control board and function generators.

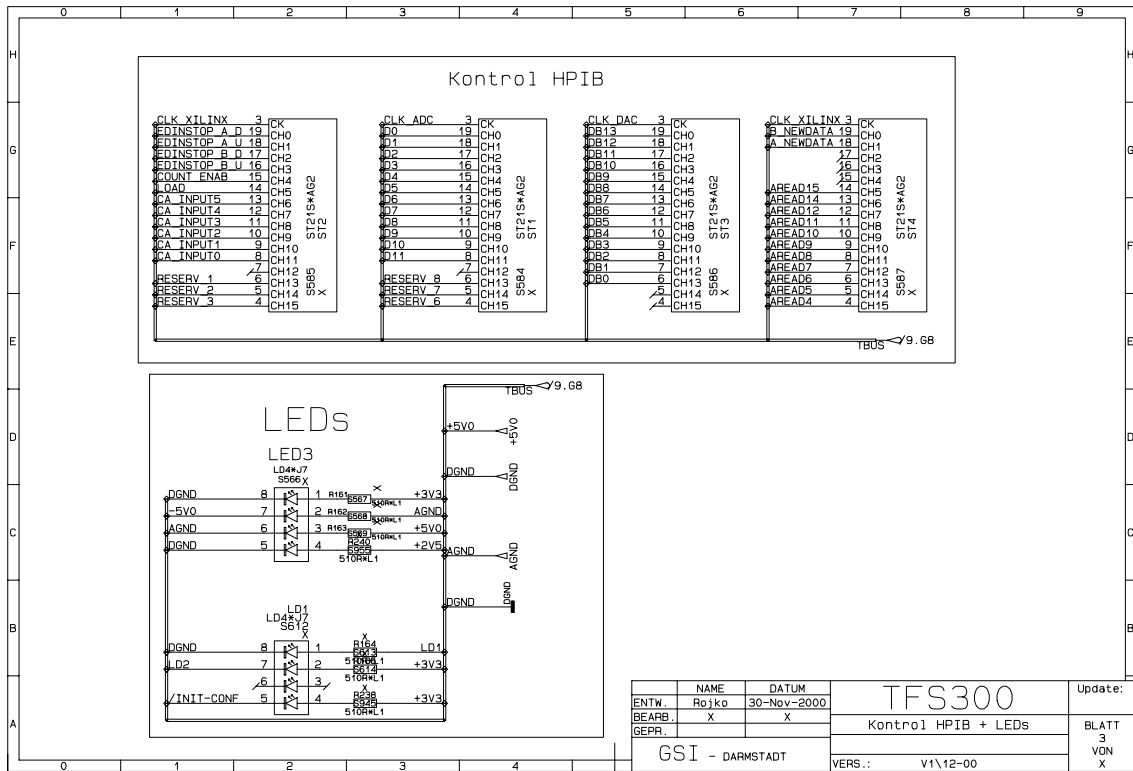


Figure C.3: Part for checking and controlling board.

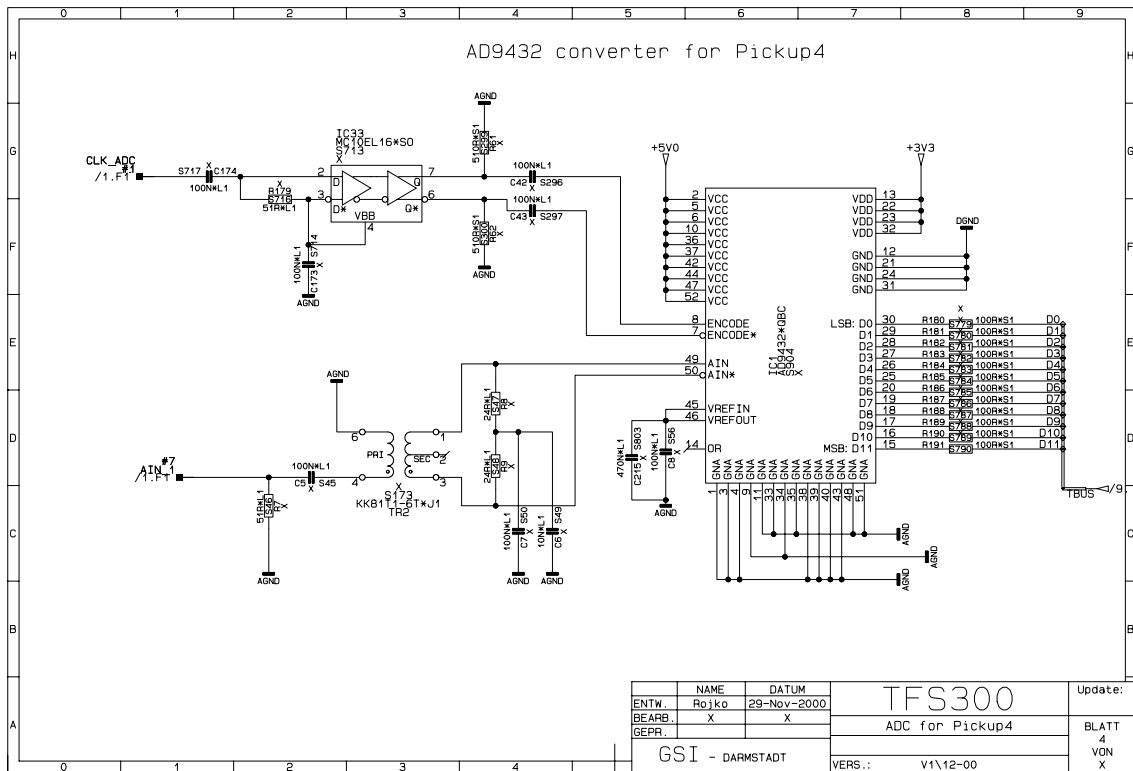


Figure C.4: Input ADC for the pickup S04DX5H or S04DX5V.

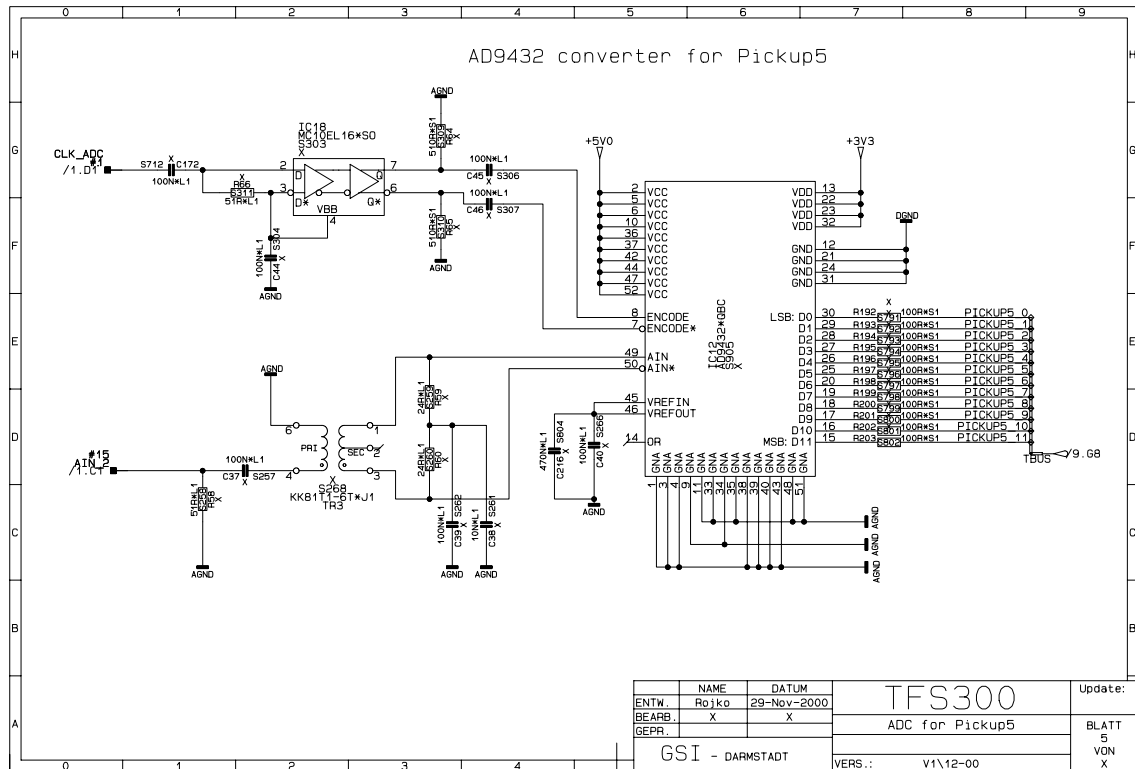


Figure C.5: Input ADC for the pickup S05DX5H or S05DX5V.

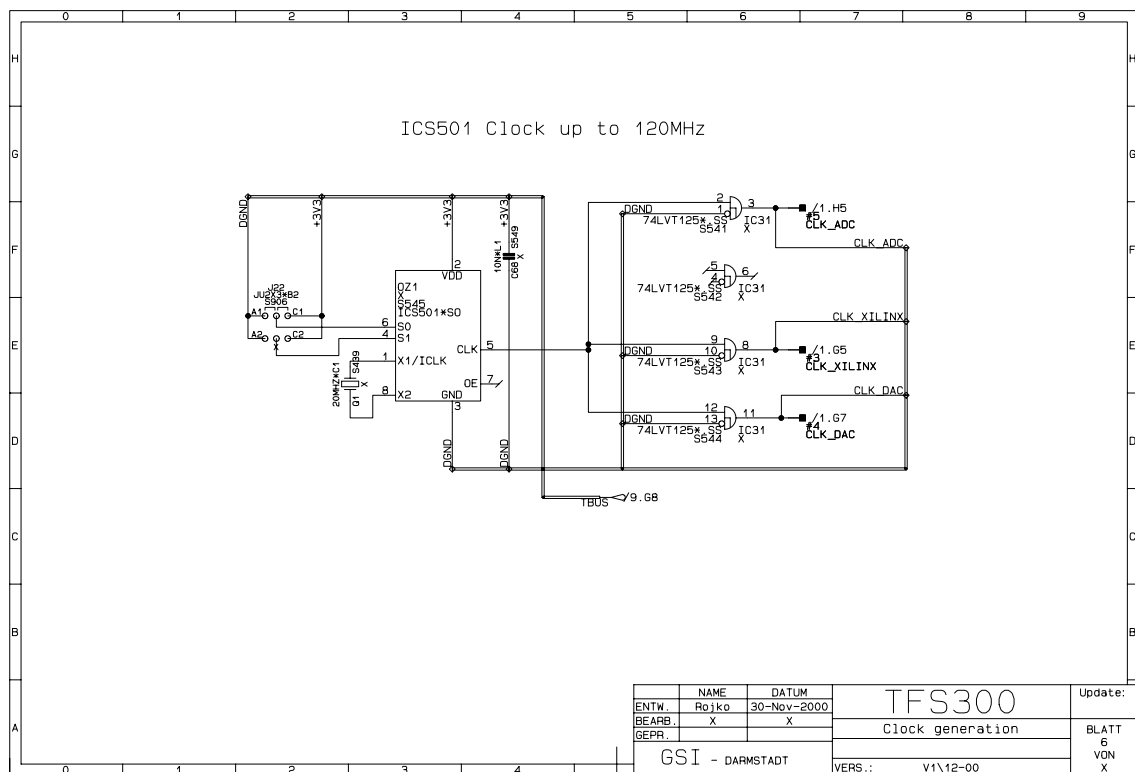


Figure C.6: Clock generation with clock distribution.

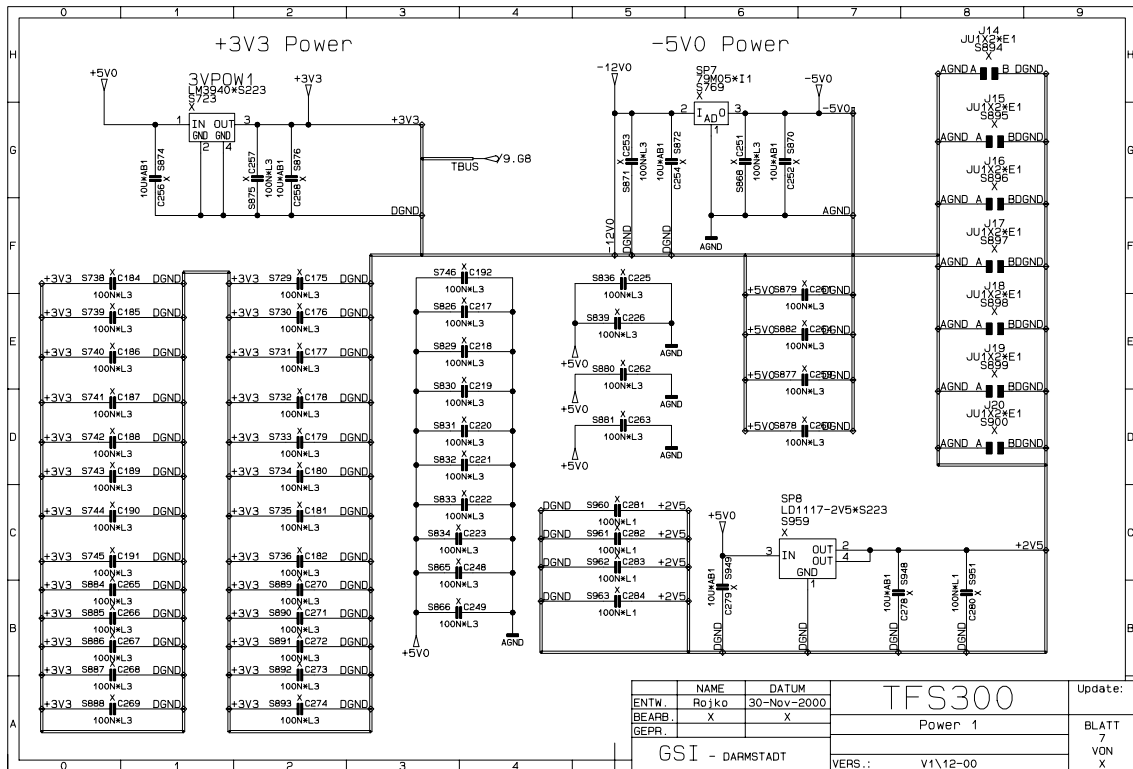


Figure C.7: Power source +3V3, +2V5 and -5V0 for the main card.

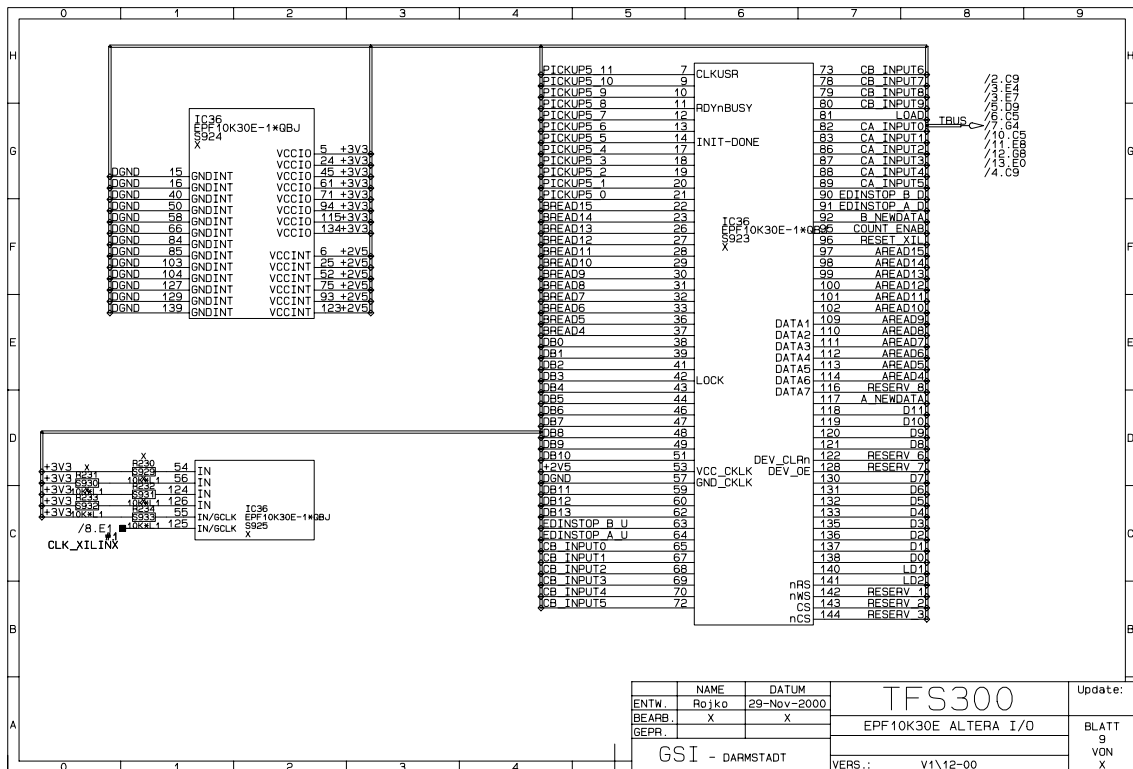


Figure C.8: ALTERA chip EPF10K30E.

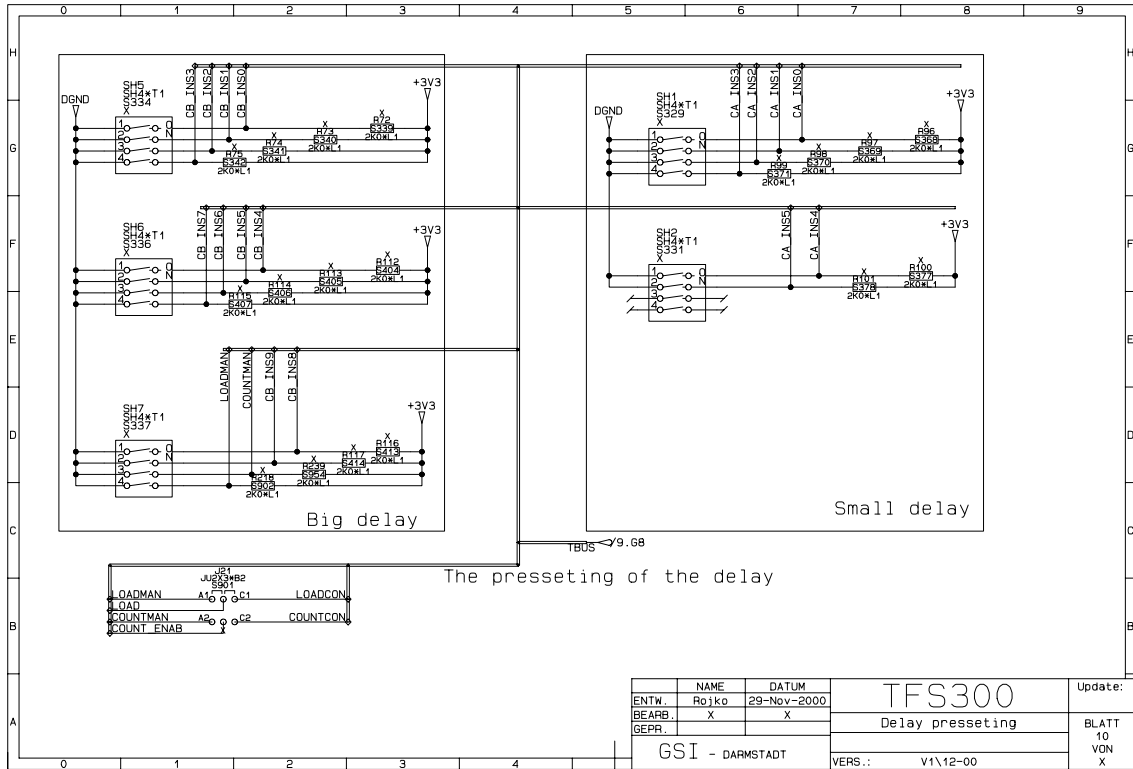


Figure C.9: Switches for presetting of the variable delay.

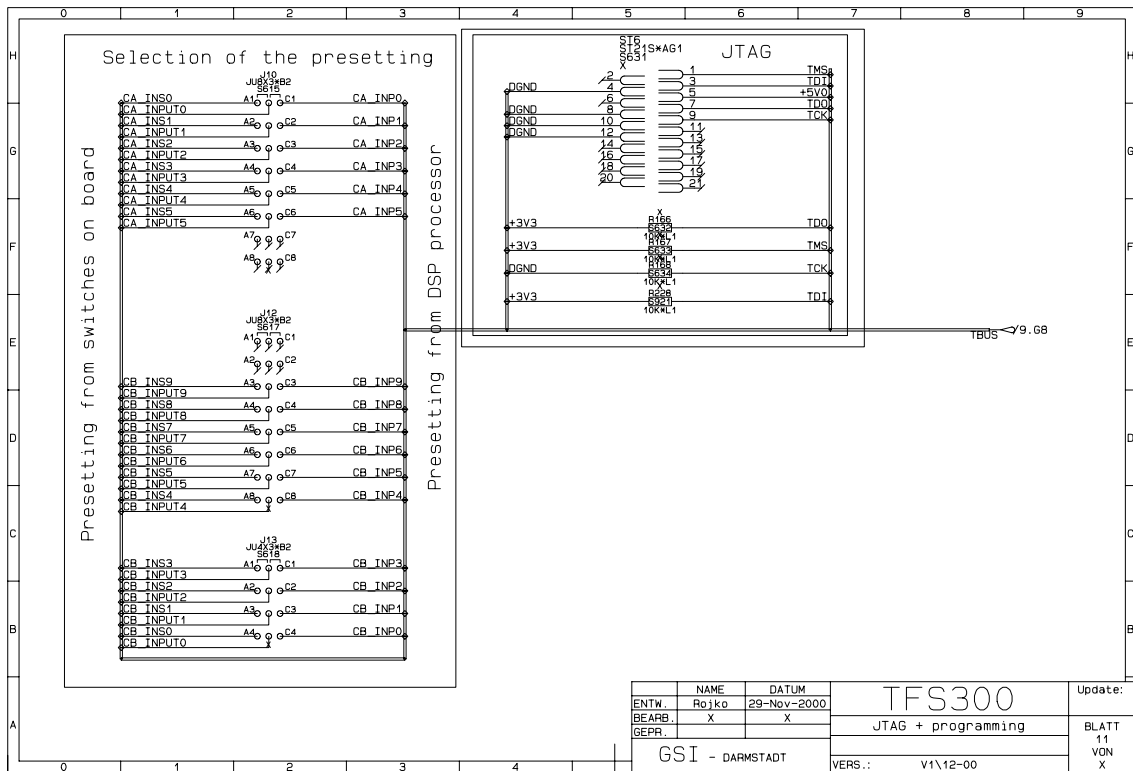


Figure C.10: Selection of the presetting: control board or 'free' run.

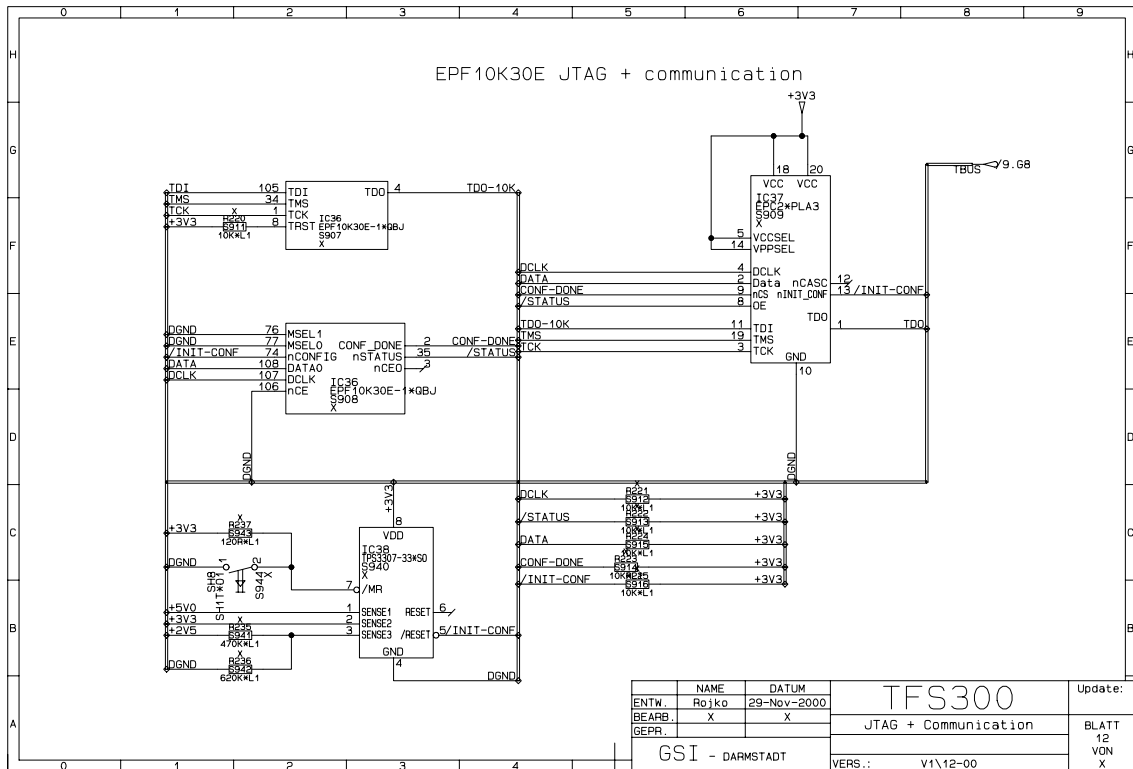


Figure C.11: JTAG communication and bootable memory.

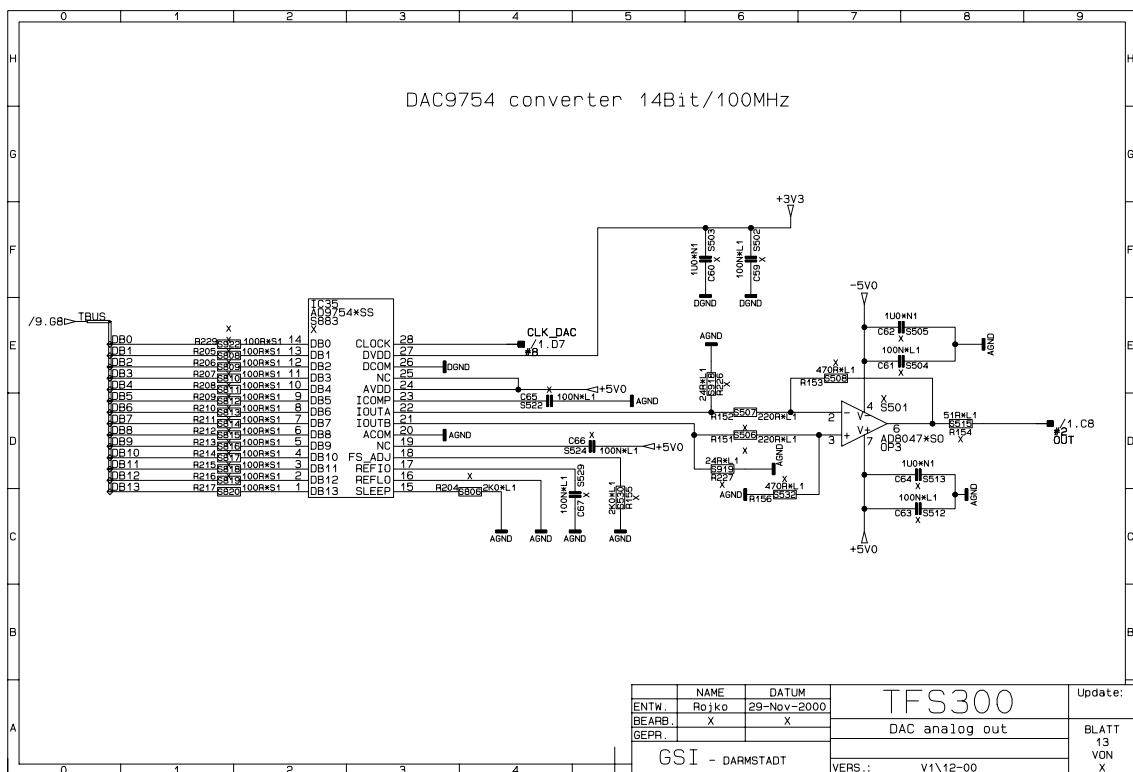


Figure C.12: Output ADC convertor.

Appendix D

Connection diagrams - Control card

Jumper description	
J4, J5	Clock frequency osillator
J7, J8, J9, J10	Boot for XCR3320 mode
SH3, SH4, SH5	Configuration switches for DSP
J12, J13, J14	Connection between DGND and PDGND
J11	Connection for external EMULATOR Reset
LED1,LED2	LED signalisation of voltages, signals ...

Table D.1: Signals description for the control board.

J4	J5	
clockmode1	clockmode0	clk
0	0	4x
0	M	5.3125x
0	1	5X
M	0	6.25X
M	M	2X
M	1	3.125X
1	0	6X
1	M	3X
1	1	8X
0 = connect directly to ground 1 = connect directly to VDD M = leave unconnected (floating) Input clock frequency = 20MHz		

Table D.2: Clock frequency for the oscillator ICS501.

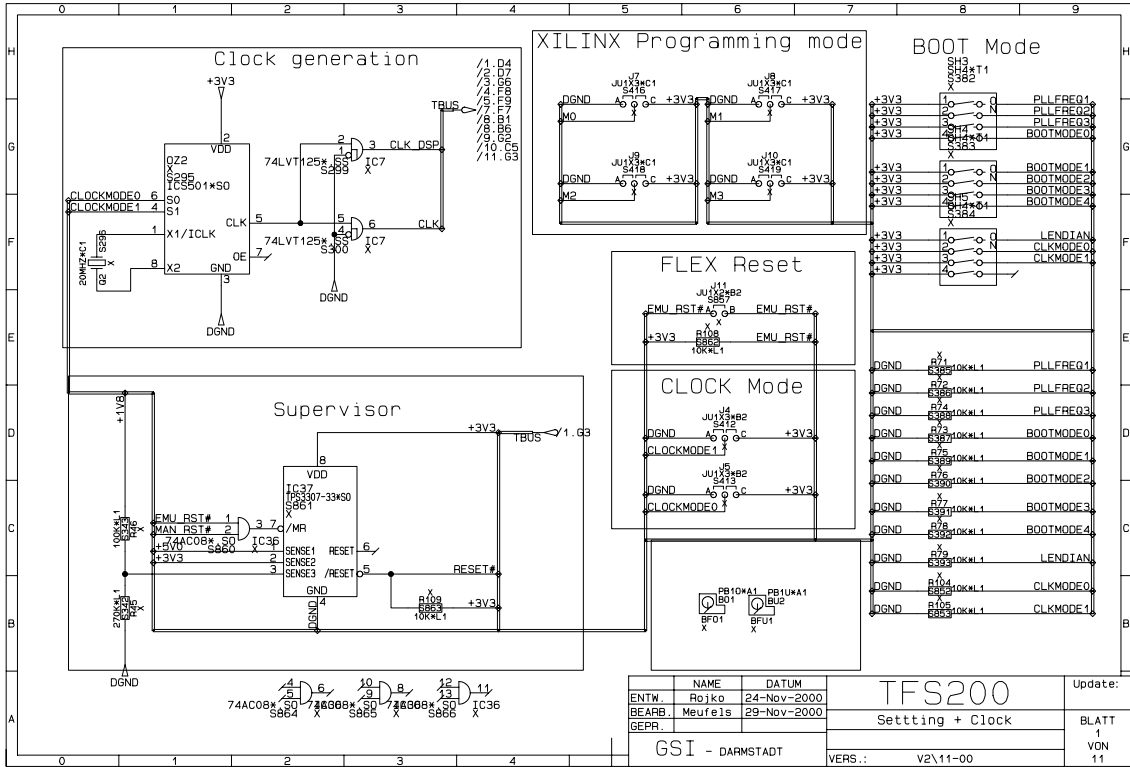


Figure D.1: The supervisor, clock generation and programming mode.

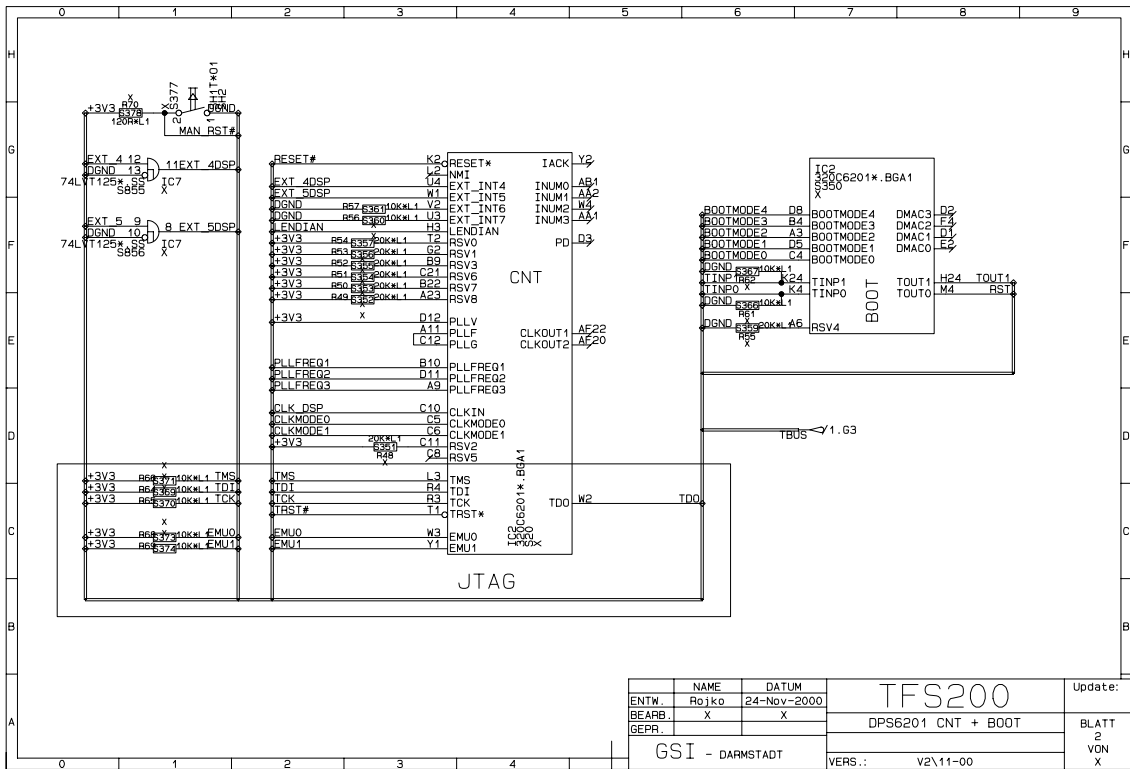


Figure D.2: The interrupt, JTAG and boot parts of the DSP processor.

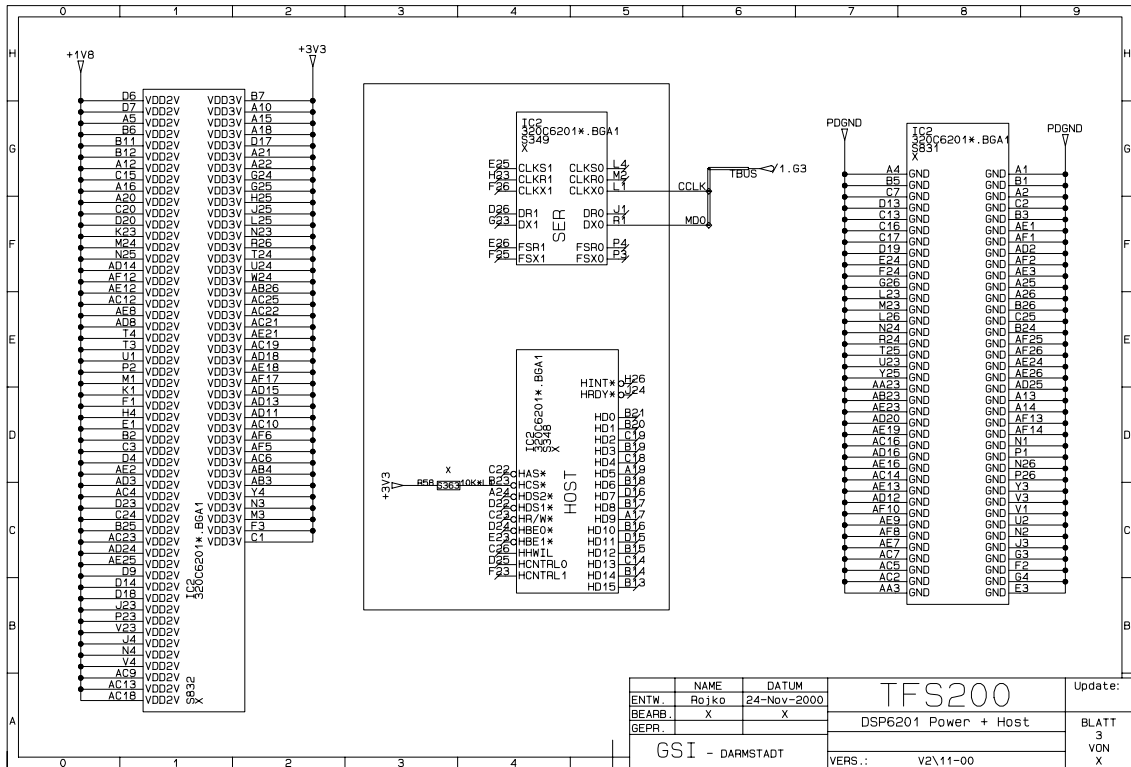


Figure D.3: DSP power and host communication.

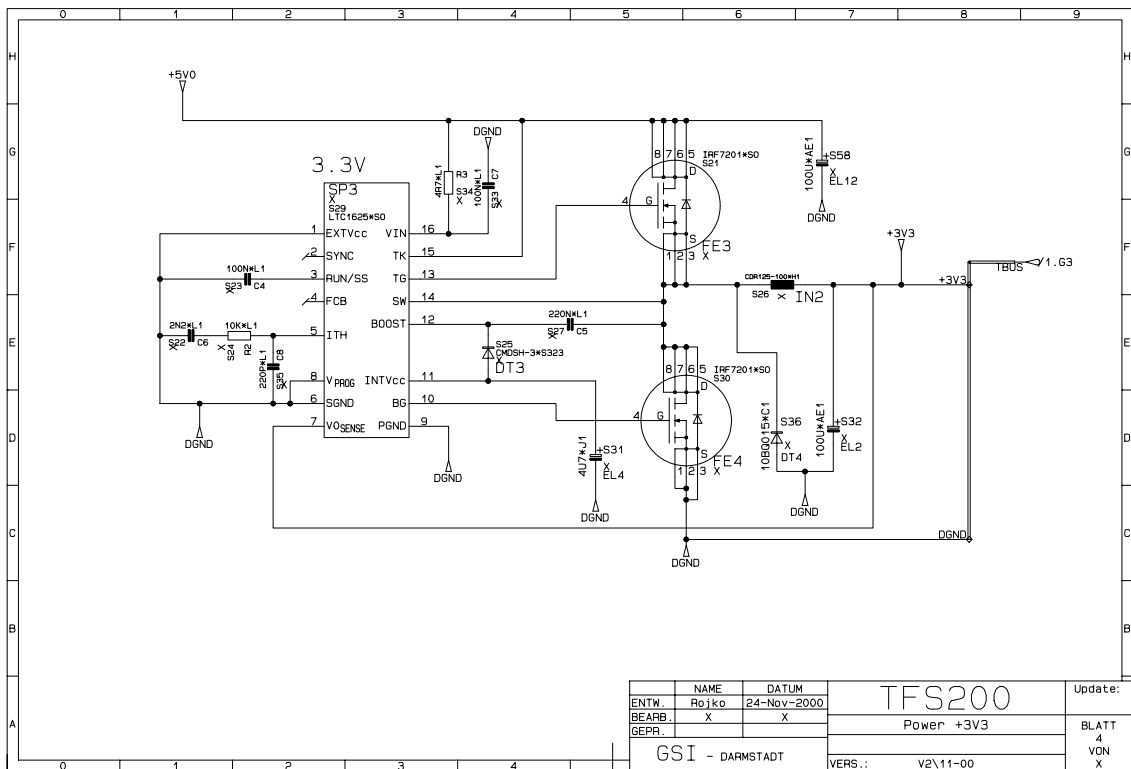


Figure D.4: Switching power supply circuit for +3V3.

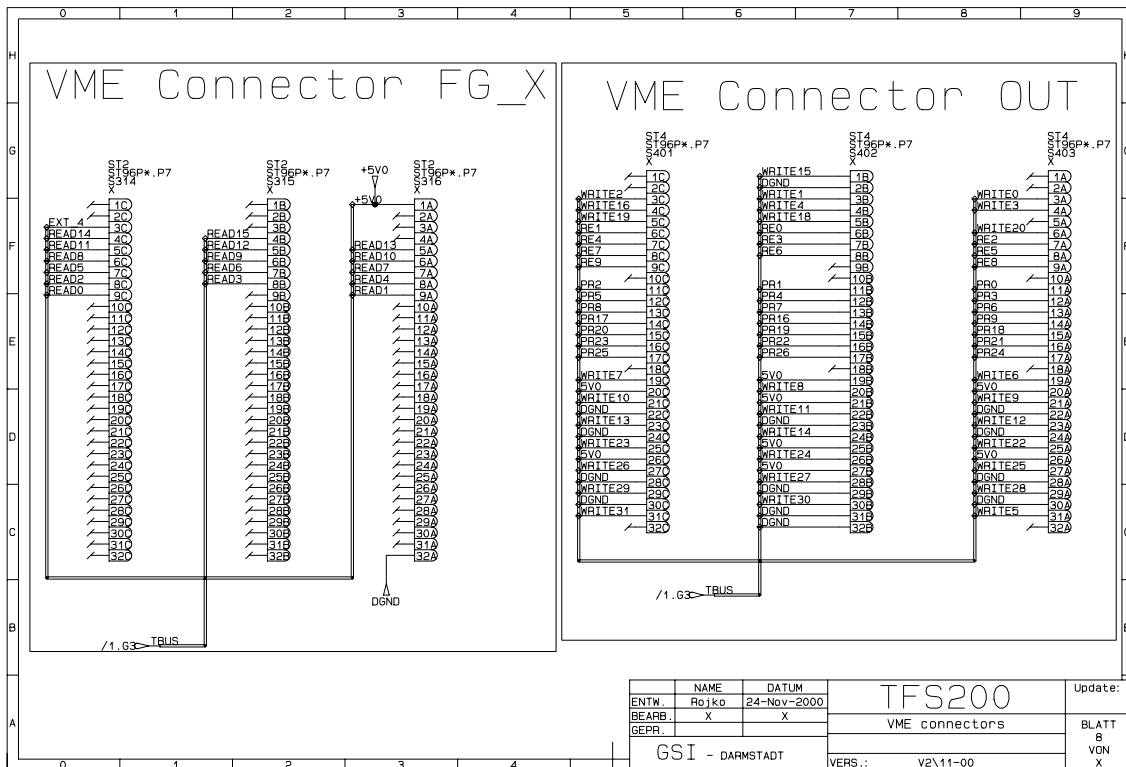


Figure D.7: The VME connectors for connection to control board and function generators.

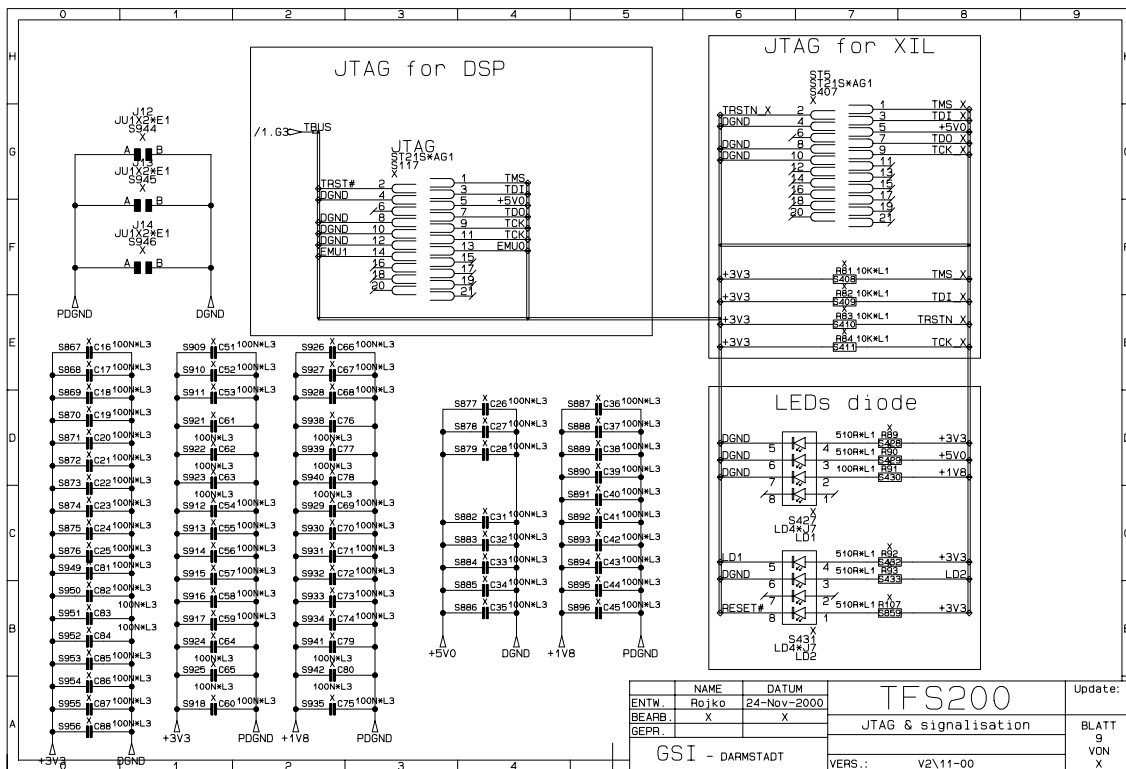


Figure D.8: JTAG for DSP and JTAG for XILINX together with signalisation.

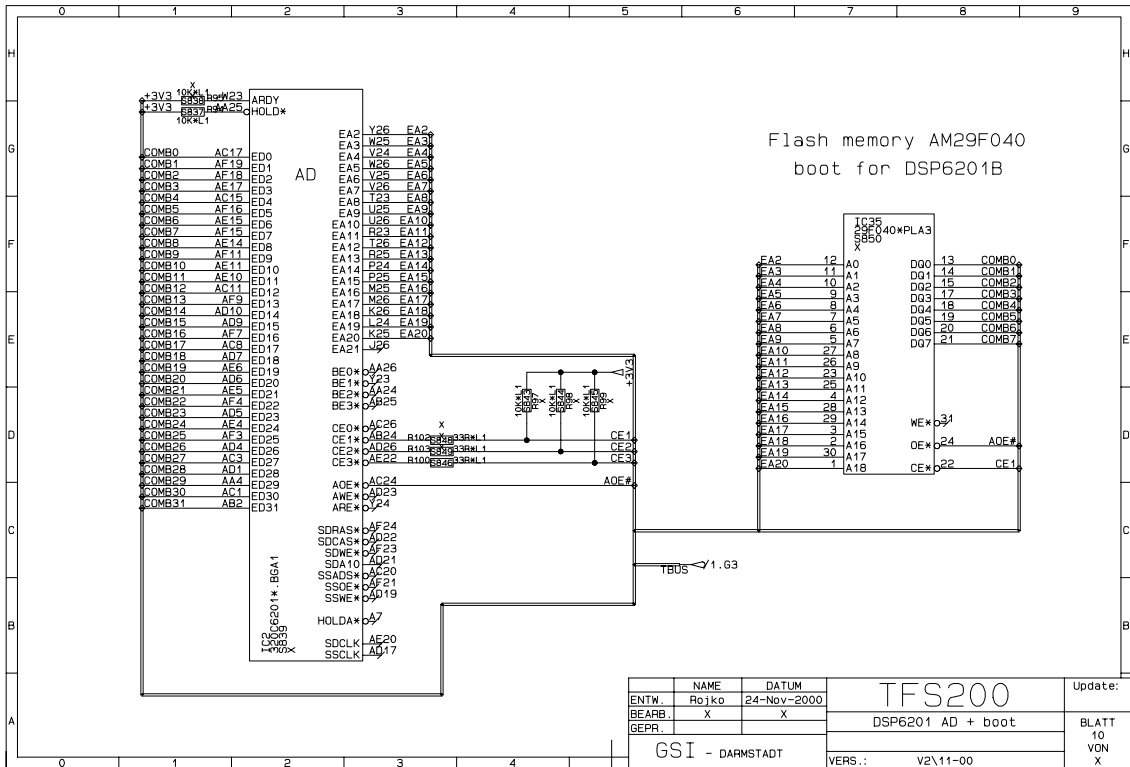


Figure D.9: DSP address and data buses with boot memory for DSP.

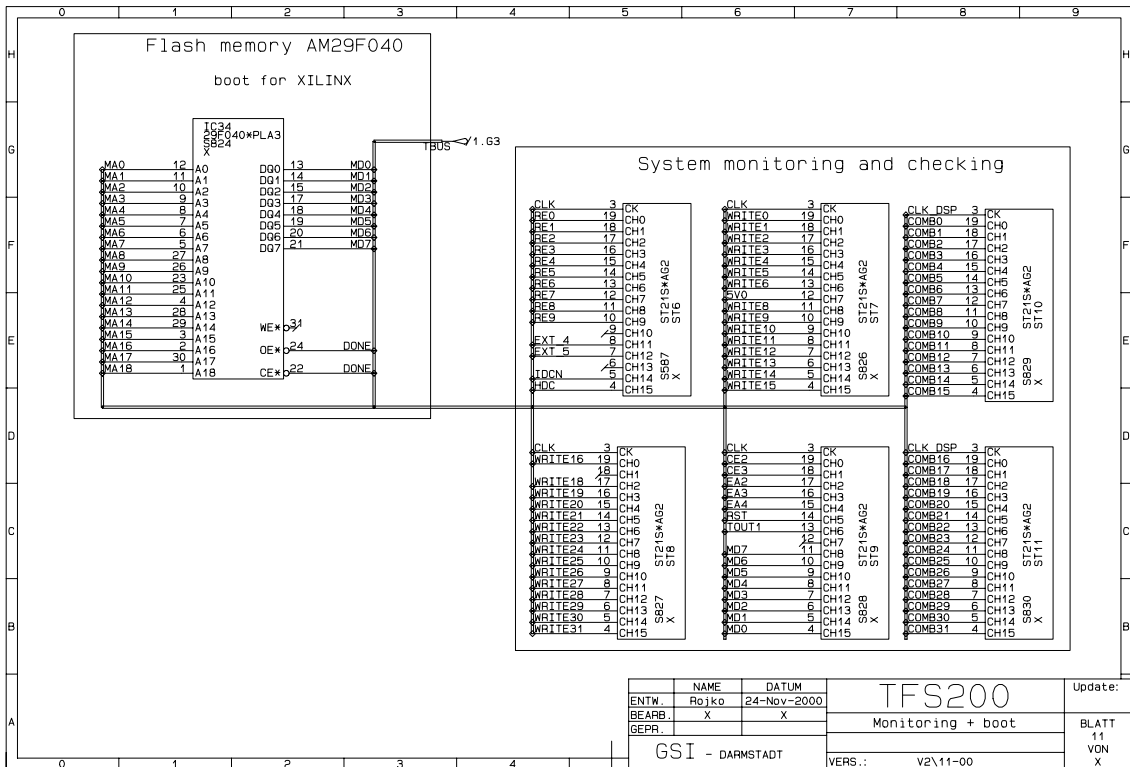


Figure D.10: Interfaces for checking and monitoring with boot memory for XILINX.

J10	J9	J8	J7			
M3	M2	M1	M0	clk	CONFIGURATION MODE	DATA FORMAT
1	0	0	0	Output	Master serial	Serial
1	0	0	1	Input	Slave parallel	Parallel
1	0	1	1	Input	Synchronous peripheral	Parallel
1	1	0	0	Output	Master parallel & up	Parallel
1	1	1	1	Input	Slave serial	Serial

Table D.3: Booting modes description for control board.

J12	J13	J14	
GND	GND	GND	connection between DGND and PDGND

Table D.4: Ground connections for control board.

	Pins	Function	Default	Description
SH3	1-2	PLLFREQ1	OFF	C6201B CLKOUT1 50-140 MHz
	3-4	PLLFREQ2	OFF	
	5-6	PLLFREQ3	OFF	
SH4	7-8	BOOTMODE0	ON	MAP1 Internal RAM, 8-bit ROM
	9-10	BOOTMODE1	OFF	
	11-12	BOOTMODE2	ON	
	13-14	BOOTMODE3	ON	
SH5	15-16	BOOTMODE4	OFF	1' little - or '0' big - endian mult x 1 f(CLKOUT)=f(CLKIN)
	17-18	LENDIAN	ON	
	19-20	CLKMODE0	OFF	
	21-22	CLKMODE1	OFF	
	23-24	*** Not Used ***	XXX	not connected
On the board: A - 1 (DGND) C - 0 (+3V3)				

Table D.5: Configuration switches description for control board.

	LD1	notes	LD2	notes
1	not used		Reset	
2	+1V8		not used	
3	+5V0		LD2_	for debugging +3V3
4	+3V3		LD1_	for debugging DGND

Table D.6: Description of LEDs signalisation.

List of Figures

2.1	Overview of the heavy ion synchrotron SIS [50].	6
2.2	Horizontal and vertical $\beta_x(s)$ and $\beta_y(s)$ betatron functions along one period in the SIS. Dashed and solid lines indicate doublet and triplet focusing modes respectively [50].	8
2.3	Phase ellipse of the particle movement in the horizontal direction [37, 131, 132].	9
2.4	α betatron functions at the exciter and pickup positions for both x and y directions.	11
2.5	β betatron functions at the exciter and pickup positions for both x and y directions.	11
3.1	Real part of the calculated transverse kicker impedance in SIS [21].	17
3.2	Imaginary part of the calculated transverse kicker impedance in SIS [21].	17
3.3	Schematic model of transverse pick-up (for horizontal direction).	18
3.4	Schematic representation of transverse beam impedance by a two electrodes.	19
3.5	Schematic design of the capacitive pick-up (a) and representation of single-plate (b).	20
3.6	Schematic model of transverse exciter.	21
3.7	Schematic representation of a pair of stripline electrodes(vertical direction).	21
3.8	A photograph of SIS exciter in the beam pipe (vertical plane). The new exciter was installed in the ring at the end of year 2000.	22
3.9	Real part of $Z_{\perp,x}^{\text{FB}}$ in horizontal direction. Calculations were done for loop gain $G = 1$	24
3.10	Imaginary part of $Z_{\perp,x}^{\text{FB}}$ in horizontal direction. Calculations were done for loop gain $G = 1$	24
3.11	Stability boundary and rise time trajectories in an dimensionless impedance plane for a beam with a parabolic momentum distribution function.	28
3.12	Stability boundary and rise time trajectories in an dimensionless impedance plane for a beam with a quartic momentum distribution function.	29
3.13	Stability boundary and rise time trajectories in an dimensionless impedance plane for a beam with a parabolic amplitude distribution function.	30
3.14	Real part of the transverse coupling impedance seen by the beam at injection energy 11.4 MeV/u ($\beta = 0.156$).	32
3.15	Imaginary part of the transverse coupling impedance seen by the beam at injection energy 11.4 MeV/u ($\beta = 0.156$).	32
3.16	Stability boundary and rise time trajectories for the SIS $^{238}\text{U}^{72+}$ beam with $3 \cdot 10^{10}$ particles at the injection energy level and without electron cooling.	34
3.17	The rise times for the SIS $^{238}\text{U}^{72+}$ beam with $3 \cdot 10^{10}$ particles at the injection energy level and without electron cooling.	34

3.18	Stability boundary and rise time trajectories for the SIS $^{238}\text{U}^{72+}$ beam with $3 \cdot 10^{10}$ particles after acceleration.	36
3.19	The rise times for the SIS $^{238}\text{U}^{72+}$ beam after acceleration.	37
4.1	Principal scheme of a classical transverse feedback system. The phase advance of the betatron oscillation is $n \times 90^\circ$ (n is odd integer) between pickup and exciter.	40
4.2	Step identification: efficiency of the feedback system.	47
4.3	Acceleration process in the worst case scenario in the SIS	49
4.4	The kick angle received by an ion going through the exciter system. The different curves represent different time errors for the $\Delta\tau = 0$ ns, 1 ns and 5 ns and $\Delta\mu = 90^\circ$	50
4.5	Parameters definition for simulation of the TFS damping rate.	55
4.6	Simulated damping methods (for injection and coasting beam) with different kicking methods. The calculated amplitude at virtual pick-up position PU3 is displayed vs time.	57
4.7	Simulations for different kicking methods. The amplitude was simulated at virtual pickup position PU3.	59
4.8	Simulation of the damping rate for $\Delta\mu = 90^\circ, 60^\circ, 40^\circ$ and 20° for a) proportional kick, b) constant kick with 10% of maximum power and c) constant kick with 100% of maximum power.	60
4.9	Simulation of the damping rate for $n = 4$ and $n = 200$ for different $\Delta\mu$ with proportional kicking.	61
4.10	Simulation of the damping time as a function of frequency for two values of time difference between particle flight time and electronic signal transit time from pickup to exciter.	62
4.11	Calculation of the maximum frequency for damping action of the TFS for two different exciter lengths $l_k = 15$ cm and $l_k = 75$ cm as a function of time difference between particle flight time and electronic signal transit time from pickup to exciter.	62
4.12	Simulation of the damping rate as a function of the system gain for different phase advances $\Delta\mu$ between "virtual" pickup PU3 and exciter.	63
5.1	Principal scheme of the main and control card [97].	68
5.2	Simulation results for real-time floating sign multiplication 12·12 bit words with coding for converters.	69
5.3	Dual port memory used for the clock signal splitting.	71
5.4	The clock splitting simulation for dual port memory.	71
5.5	Delay line switches with three bits.	72
5.6	Practical realisation of long, short, and fine delays.	72
5.7	The simulation results for digital part of the TFS implemented in the 30KE. The "30KE new" version was simulated with flip-flops at each digital input and output.	73
5.8	Measured delay vs. programmed delay.	76
5.9	Distribution of differential delay steps.	77
5.10	Integral deviation of the delay value from its nominal value.	77
5.11	The measured phase characteristic of the digital system for the time delay $T_{\text{delay}} = 0.5 \mu\text{s}$ in the frequency range from 20 kHz to 50 MHz. The phase error is only $\pm 2^\circ$. (2 degree/division)	78

5.12	The measured phase characteristic of the digital system for the time delay $T_{\text{delay}} = 2.5 \mu\text{s}$ in the frequency range from 20 kHz to 50 MHz. The phase error is only $\pm 2^\circ$. (2 degree/division)	79
5.13	The measured phase characteristic of the combined digital and analogue systems for the time delay $T_{\text{delay}} = 1.3 \mu\text{s}$ in the frequency range from 20 kHz to 50 MHz. The phase error is only $\pm 4^\circ$. (2 degree/division)	79
5.14	The measured amplitude characteristic of the combined digital and analogue systems for the time delay $T_{\text{delay}} = 1.3 \mu\text{s}$ in the frequency range from 20 kHz to 50 MHz.	80
5.15	Delay line for generation of a periodic notch filter structure with feedback factor $0.0 \leq b_{\text{par}} \leq 1.0$	81
5.16	Amplitude of a periodic notch filter structure with feedback factor $0.0 \leq b_{\text{par}} \leq 1.0$ in the frequency range from 5 MHz to 10 MHz.	82
5.17	Amplitude characteristic (5 dB/division) for the time dependent notch filter in the frequency range from 20 kHz to 50 MHz. The set value $f_{\text{notch}} = 500$ kHz. The frequency range from 2 MHz to 15 MHz is characterised by a notch depth of up to 35 dB.	82
5.18	Phase characteristic for a variable notch filter in the frequency range from 20 kHz to 50 MHz. The set value $f_{\text{notch}} = 500$ kHz.	83
5.19	Design of the transverse feedback system	84
5.20	Structure of the control system for controlling the TFS in the SIS.	87
6.1	Arrangement to measure beam transfer function. The frequency sweep of the network analyser is set to cover one or several betatron sidebands.	90
6.2	Vertical lower and upper betatron sidebands for the 163th harmonics of a $^{86}\text{Kr}^{34+}$ beam at the injection energy of 11.4 MeV/u. Due to coherent instabilities the transverse sidebands can increase.	90
6.3	Pickup measurements in the frequency domain. The upper plot shows response of the Schottky pickup in the frequency range up to 30 MHz. The lower plot represents the same measurement with position pickup DX1.	91
6.4	The effect of the solenoid magnet of the Electron-cooler on the 5th harmonic. Measured values of the tunes are $Q_y = 3.27$ and $Q_x = 4.32$	92
6.5	The ‘‘artificial’’ coherent instabilities were produced by electron cooler and the TFS was switched on. The measurement with the TFS was reproduced three times. (the TFS was switched on and off 3 times.) (Measurement was done in the ESR.)	95
6.6	Methods for pre-commissioning of the TFS. The measured natural damping time is approximately 136 ms. (Measurement were done in the SIS.)	96
6.7	Lower (1) and upper (3) betatron coherent sidebands in the horizontal direction for the 20th harmonics of a $^{197}\text{Au}^{65+}$ beam at the extraction energy of 350 MeV/u. In the center $f=19,00155$ MHz (2) is the longitudinal signal.	98
6.8	An example of the measured spectrum of the signal generator on the flat top for knock-out measurements in the frequency range from 100 kHz to 5 MHz.	99
6.9	Two characteristics represent the relative amplitudes of the noise generation (KNOCK-OUT) and of the current transformer. The four phases specify: A - accumulation phase, B - acceleration phase, C - flat-top phase with the slow extraction and D - start and stop phase of the accelerator cycle.	100
6.10	Results from measurement in the horizontal direction in the SIS. The different input conditions are listed in the table 6.1.	101

B.1	The entire feedback integrated in the ALTERA chip EPF10K30ETC144-1.	113
B.2	Memory implementation with automatically running counters in the ALTERA chip EPF10K30ETC144-1.	114
B.3	Implementation of the multiplication with decoding in the ALTERA chip EPF10K30ETC144-1.	115
B.4	Data flow diagram for the control card.	116
C.1	The principal scheme of the main card presented in modules.	118
C.2	The VME connectors for connection to control board and function generators.	118
C.3	Part for checking and controlling board.	119
C.4	Input ADC for the pickup S04DX5H or S04DX5V.	119
C.5	Input ADC for the pickup S05DX5H or S05DX5V.	120
C.6	Clock generation with clock distribution.	120
C.7	Power source +3V3, +2V5 and -5V0 for the main card.	121
C.8	ALTERA chip EPF10K30E.	121
C.9	Switches for presetting of the variable delay.	122
C.10	Selection of the presetting: control board or 'free' run.	122
C.11	JTAG communication and bootable memory.	123
C.12	Output ADC convertor.	123
D.1	The supervisor, clock generation and programming mode.	126
D.2	The interrupt, JTAG and boot parts of the DSP processor.	126
D.3	DSP power and host communication.	127
D.4	Switching power supply circuit for +3V3.	127
D.5	Switching power supply circuit for +1V8.	128
D.6	XILINX chip for communication between DSP and ALTERA.	128
D.7	The VME connectors for connection to control board and function generators.	129
D.8	JTAG for DSP and JTAG for XILINX together with signalisation.	129
D.9	DSP address and data buses with boot memory for DSP.	130
D.10	Interfaces for checking and monitoring with boot memory for XILINX.	130

List of Tables

1.1	Some parameters of various transverse feedback systems. Most of these systems are working at $\beta \approx 1$ [35, 85].	3
2.1	Beam and ring parameters [50].	7
3.1	Some formulaes for contribution to coupling impedance's Z_{\perp}	16
3.2	Parameters of the pick-up and exciter.	20
3.3	Specific beam and machine parameters.	31
3.4	Calculation of the growth rate and stability at injection energy ($\beta = 0.158$) for coasting beam.	35
3.5	Calculation of the growth rate and stability after acceleration of the beam ($\beta = 0.58$).	37
4.1	Specific parameters of the transverse feedback system.	46
4.2	The time delay per turn for a particle with relative momentum deviation $\frac{\delta p}{p}$ for two different β values and momentum deviations.	48
4.3	Key parameters for the variable delay system.	48
4.4	Comparison of delay line technologies [5, 8, 35, 89, 90, 91].	52
6.1	The evaluation of the TFS efficiency with the beam. In the column "plot" the TFS_1, TFS_2, TFS_3, and TFS_4 corresponds to plots in the figure 6.10.101	
D.1	Signals description for the control board.	125
D.2	Clock frequency for the oscillator ICS501.	125
D.3	Booting modes description for control board.	131
D.4	Ground connections for control board.	131
D.5	Configuration switches description for control board.	131
D.6	Description of LEDs signalisation.	131

Bibliography

- [1] "Digital signal processing in FLEX Devices," *ALTERA Corporation, Product Information Bulletin 23, A-PIB-023-01, 1996 8 p.*
- [2] "MAX+PLUSII Getting Started," *ALTERA Corporation, Manual P25-04803-03, 1997 380 p.*
- [3] "High-Speed Board Designs," *ALTERA Corporation, Application note 75, A-AN-075-03.01, 1999 15 p.*
- [4] "FLEX10KE Embedded Programmable Logic Family," *ALTERA Corporation, Data Sheet, A-DS-F10KE-02.02, 1999 121 p.*
- [5] L. Andrew, "ACT Technology Bestows Accelerated Signal Processing," *Microwaves & RF, Vol. 28, No. 8, August 1989.*
- [6] N. Angert, "Ion Accelerators And Storage Rings," *C88-06-07 Prepared for 1st European Particle Accelerator Conference (EPAC 88), Rome, Italy, 7-11 Jun 1988.*
- [7] N. Angert, "Status And Future Prospect Of Unilac And Sis / Esr," *In *Tokyo 1990, Proceedings, Physics with high intensity hadron accelerators* 417-431.*
- [8] K. Balewski, "Review of feedback systems," *DESY-M-98-06A Prepared for 6th European Particle Accelerator Conference (EPAC 98), Stockholm, Sweden, 22-26 Jun 1998.*
- [9] W. Barry, J. M. Byrd, J. N. Corlett, J. Hinkson, J. Johnson, G. R. Lambertson and J. D. Fox, "Design of the ALS transverse coupled-bunch feedback system," *LBL-33269 1993 Particle Accelerator Conference (PAC 93), Washington, DC, 17-20 May 1993.*
- [10] W. Barry, G. R. Lambertson and C. C. Lo, "Electronic systems for transverse coupled bunch feedback in the Advanced Light Source (ALS)," *SLAC-PEP-II-AP-NOTE-39-93 Submitted to Beam Instrumentation Workshop, Santa Fe, NM, Oct 20-23, 1993.*
- [11] W. Barry, J. Byrd, J. Corlett, G. R. Lambertson and C. C. Lo, "Transverse coupled bunch feedback in the advanced light source (ALS)," *LBL-34953 Presented at 4th European Particle Accelerator Conference (EPAC 94), London, England, 27 Jun - 1 Jul 1994.*
- [12] W. Barry, J. Byrd, J. Corlett, J. Johnson, G. Lambertson and J. Fox, "Commissioning of the ALS transverse coupled-bunch feedback system," *In *Dallas 1995, PAC, vol. 4* 2423-2425.*
- [13] W. Barry *et al.*, "Design of the PEP-II transverse coupled bunch feedback system," *SLAC-PEP-II-AP-NOTE-95-09 Contributed to 16th IEEE Particle Accelerator Conference (PAC 95) and International Conference on High Energy Accelerators (IUPAP), Dallas, Texas, 1-5 May 1995.*
- [14] W. Barth *et al.*, "Commissioning of Ih-RFQ and Ih-DTL for the Gsi High Current Linac," in , physics/0008136.

-
- [15] J. S. Berg, "Coherent modes for multiple nonrigid bunches in a storage ring," SLAC-R-0478.
- [16] F. Blas and R. Garoby, "Automatic Delay Compensation," *CERN/PS/RF/Note 95-05, February 1995*
- [17] K. Blasche and D. Bohne, "Status Report On The Gsi Synchrotron Facility And First Beam Results," *Prepared for IEEE Particle Accelerator Conference, Chicago, IL, 20-23 Mar 1989.*
- [18] K. Blasche, D. Bohne, H. Eickhoff, B. Franczak, B. Franzke, H. Prange and R. Steiner, "Status Of The Sis/Esr-Facility At Gsi Darmstadt," *Part. Accel.* **32** (1990) 83.
- [19] K. Blasche, B. Franczak, B. Langenbeck, G. Moritz and C. Riedel, "The heavy ion synchrotron SIS: A progress report," *Prepared for 1993 IEEE Particle Accelerator Conference (PAC 93), Washington, DC, 17-20 May 1993.*
- [20] K. Blasche, B. Franczak, K. Kaspar, P. Moritz and U. Oeftiger, "SIS operation at high beam intensities," *Darmstadt GSI - GSI-Nachr.-95-12 (95,rec.Jan.96) 17-24.*
- [21] U. Blell, "Measurement of the kicker coupling impedances in the SIS and ESR at GSI," *Prepared for 1998 IEEE Particle Accelerator Conference (PAC 98), New York, 17-20 April 1998, 1727-1728.*
- [22] D. Bohne, K. Blasche, B. Franzke and H. Prange, "Status Report On The Sis / ESR Project At Gsi," *Nucl. Instrum. Meth.* **A278** (1989) 19.
- [23] D. Briggs *et al.*, "Computer modeling of bunch by bunch feedback for the SLAC B factory design," SLAC-PUB-5466 *Presented at IEEE Particle Accelerator Conf., San Francisco, CA, May 6-9, 1991.*
- [24] R. Bossart, R. Louwerse, J. Mourier and L. Vos, "Operation of the transverse feedback system at the CERN SPS," *Prepared for 12th Particle Accelerator Conference (PAC), Washington, DC, 16-19 Mar 1987.*
- [25] D. Boussard, "Schottky noise and beam transfer function diagnostics," *Prepared for CERN Accelerator School: Course on Advanced Accelerator Physics (CAS), Rhodes, Greece, 20 Sep - 1 Oct 1993.*
- [26] P. J. Bryant, "A Brief history and review of accelerators," *In *Jyvaeskylae 1992, Proceedings, General accelerator physics, vol. 1* 1-16. CERN Geneva - CERN-94-01 (94/01,rec.Mar.) 1-16.*
- [27] P. J. Bryant, "Insertions," *In *Jyvaeskylae 1992, Proceedings, General accelerator physics, vol. 1* 159-190. CERN Geneva - CERN-94-01 (94/01,rec.Mar.) 159-190.*
- [28] P. J. Bryant, "Beam transfer lines," *In *Jyvaeskylae 1992, Proceedings, General accelerator physics, vol. 1* 219-238. CERN Geneva - CERN-94-01 (94/01,rec.Mar.) 219-238.*
- [29] P. J. Bryant and K. Johnsen, "The Principles of circular accelerators and storage rings," *Cambridge, UK: Univ. Pr. (1993) 357 p.*
- [30] D. Bulfone *et al.*, "Design considerations for the ELETTRA transverse multi-bunch feedback," *In Proceedings of the 1999 PAC, New York, 1999, 1120-1122.*
- [31] J. M. Byrd and F. Caspers, "Spectrum and network analyzers," *CERN-PS-99-003-RF CAS -CERN Accelerator School : Beam Measurement, Montreux, Switzerland, 11 -19 May 1998.*
- [32] F. Caspers, "Experience with stochastic cooling of particle beams," *CERN-PS-97-013 International Symposium on Multi-GeV Higgs Performance Accelerators and Related Techniques, Osaka, Japan, 12 -14 Mar 1997.*

-
- [33] F. Caspers, M. Chanel and U. Oeftiger, "A novel method of noise suppression in beam transfer function measurements," *Prepared for 1993 IEEE Particle Accelerator Conference (PAC 93), Washington, DC, 17-20 May 1993.*
- [34] M. Chanel, R. Maccaferri and J.C. Perrier, "Momentum Stochastic Cooling with Digital Notches," *contribution to the second EPAC, Nice 1990.*
- [35] M. Chanel, "Beam instabilities and their cures," CERN-PS-96-009-AR *31st Eloisatron Workshop on Crystalline Beams and Related Issues, Erice, Italy, 11 -21 Nov 1995.*
- [36] A. W. Chao, "Coherent Instabilities Of A Relativistic Bunched Beam," SLAC-PUB-2946 *Lectures given at 2nd Summer School on High Energy Particle Accelerators, Stanford, Calif., Aug 2-13, 1982.*
- [37] A. W. Chao, "Physics of collective beam instabilities in high-energy accelerators," *New York, USA: Wiley (1993) 371 p.*
- [38] S. Chen and G. Lopez, "Simulation studies of the transverse dipole mode multibunch instability for the SSC collider," SSCL-614.
- [39] W. Chou and J. Peterson, "Issues of the transverse feedback systems design at the SSC," SSCL-PREPRINT-414 *Presented at 1993 Particle Accelerator Conference (PAC 93), Washington, DC, 17-20 May 1993.*
- [40] W. Chou and J. Peterson, "The SSC transverse feedback systems," SSCL-623 *In *Erice 1991/1992, Proceedings, Supercolliders and superdetectors* 188-208, and SSC Dallas - SSCL-623 (93/06,rec.Jul.) 28 p.*
- [41] W. Chou, "Review of beam instability studies for the SSC," *In *Dallas 1995, PAC, vol. 5* 2983-2985.*
- [42] C. Christiansen, "Closed Orbit Signal Suppressor for the TFS of the PSB," *CERN/PS/BR.80-05.*
- [43] M. Ebert *et al.*, "Compensation of the multibunch instabilities with feedback systems," *In *Hamburg 1992, Proceedings, High energy accelerators, vol. 1* 421-423. (Int. J. Mod. Phys. A, Proc. Suppl. 2A (1993) 421-423).*
- [44] J. D. Fox, N. Eisen, H. Hindi, I. Linscott, G. Oxoby, L. Sapozhnikov and M. Serio, "Feedback control of coupled-bunch instabilities," SLAC-PUB-6180 *Presented at 1993 Particle Accelerator Conference (PAC 93), Washington, DC, 17-20 May 1993.*
- [45] J. D. Fox *et al.*, "Operation and performance of a longitudinal damping system using parallel digital signal processing," SLAC-PUB-6548 *Presented at 4th European Particle Accelerator Conference (EPAC 94), London, England, 27 Jun - 1 Jul 1994.*
- [46] J. D. Fox *et al.*, "Observation, control, and modal analysis of longitudinal coupled-bunch instabilities in the ALS via a digital feedback system," SLAC-PUB-7292 *Talk given at 7th Beam Instrumentation Workshop (BIW 96), Argonne, IL, 6-9 May 1996.*
- [47] J. D. Fox and E. Kikutani, "Bunch feedback systems and signal processing," *Prepared for Joint US-CERN-Japan-Russia School on Particle Accelerators: Beam Measurement, Montreux, Switzerland, 11-20 May 1998.*
- [48] J. Fox *et al.*, "Multi-bunch longitudinal dynamics and diagnostics via a digital feedback system at PEP-II, DAPHNE, ALS and SPEAR," SLAC-PUB-8128 *Presented at 6th European Particle Accelerator Conference (EPAC 98), Stockholm, Sweden, 22-26 Jun 1998.*
- [49] J. Fox *et al.*, "Multi-bunch instability diagnostics via digital feedback systems at PEP-II, DAPHNE, ALS and SPEAR," SLAC-PUB-8129 *Invited talk at IEEE Particle Accelerator Conference (PAC 99), New York, NY, 29 Mar - 2 Apr 1999.*

-
- [50] B. Franczak, "SIS Parameter List," *GSI-SIS-TN / 97-13 (1987)*.
- [51] R. Garoby, "Low level RF and feedback," CERN-PS-97-034 *Joint US-CERN-Japan Accelerator School, Tsukuba, Japan, 9 -18 Sep 1996*.
- [52] H. Geissel *et al.*, "The GSI projectile fragment separator (FRS): A Versatile magnetic system for relativistic heavy ions," GSI-91-46.
- [53] "PROGRAMMABLE DELAY LINE - MODEL PADL," *GIGABAUDICS Corporation, Data sheet, 1998 8 p.*
- [54] D. A. Goldberg and G. R. Lambertson, "Dynamic devices: A Primer on pickups and kickers," LBL-31664 *In *Month, M. (ed.), Dienes, M. (ed.): The physics of particle accelerators, vol. 1* 537-600.*
- [55] K. Hanaoka, "Design of a transverse feedback system against multibunch beam oscillation due to impedance in the KEK B factory rings," KEK-REPORT-95-10.
- [56] K. Hanaoka, "A Beam test of a transverse beam oscillation monitor for a multibunch beam feedback system in the KEK B," KEK-REPORT-95-13.
- [57] D. Heins, K. H. Matthiesen, S. Patzold, D. Renken and K. Wille, "The Transverse Feedback System At Petra," DESY M-79/06.
- [58] D. Heins, J. Klute, R. D. Kohaupt, K. H. Matthiesen, S. Patzold, J. Rummler and M. Schweiger, "Wide Band Multibunch Feedback Systems For Petra," DESY-89-157.
- [59] D. Heins, J. Klute, R. D. Kohaupt, K. H. Matthiesen, S. Patzold and J. Rummler, "The transverse damping system with DSP PLL tune measurement for HERA-p," DESY-M-96-21 *Talk given at the 5th European Particle Accelerator Conference (EPAC 96), Sitges, Spain, 10-14 Jun 1996.*
- [60] D. A. Herrup, D. McGinnis, J. Steimel and R. Tomlin, "Analog dampers in the Fermilab booster," *In *Dallas 1995, PAC, vol. 5* 3010-3012.*
- [61] H. Hindi, N. Eisen, J. Fox, I. Linscott, G. Oxoby, L. Sapozhnikov and M. Serio, "Analysis of DSP-based longitudinal feedback system: Trials at SPEAR and ALS," SLAC-PUB-6151 *Presented at 1993 Particle Accelerator Conference (PAC 93), Washington, DC, 17-20 May 1993.*
- [62] W. Hofle, "Towards a transverse feedback system and damper for the SPS in the LHC era," *Part. Accel.* **58** (1997) 269.
- [63] A. Hofmann, "Vlasov equation and Landau damping," *In *Noordwijkerhout 1991, Proceedings, Advanced accelerator physics* 88-99. (see HIGH ENERGY PHYSICS INDEX 30 (1992) No. 9905).*
- [64] A. Hofmann, "Landau damping," *Prepared for CERN Accelerator School: Course on Advanced Accelerator Physics (CAS), Rhodes, Greece, 20 Sep - 1 Oct 1993.*
- [65] A. Hofmann, "Beam Instabilities," *Prepared for CERN Accelerator School: Course on Advanced Accelerator Physics (CAS), Rhodes, Greece, 20 Sep - 1 Oct 1993, pp. 307-330*
- [66] A. Hofmann, "Kinetic Theory," *Prepared for CERN Accelerator School: Course on Advanced Accelerator Physics (CAS), Rhodes, Greece, 20 Sep - 1 Oct 1993, pp. 259-274*
- [67] "Benutzerhandbuch Netzwerk/Spektrum-Analysator HP 4396A," *Hewlett Packard Manual Part No. 04396-96101, Japan 1993.*
- [68] I. N. Ivanov and V. A. Melnikov, "Nonlinear damping of coherent transverse oscillations of a beam in hadron cyclic accelerators and colliders," *Nucl. Instrum. Meth. A* **391** (1997) 52.

-
- [69] E. Kikutani, T. Katsura, T. Obina, T. Kasuga and M. Tobiyama, "Bunch feedback systems," *Given at International Workshop on B Factories: Accelerators and Experiments, Tsukuba, Japan, 17-20 Nov 1992.*
- [70] E. Kikutani, T. Kasuga, Y. Minagawa, T. Obina, M. Tobiyama and L. Ma, "Development of bunch feedback system for KEK B," KEK-PREPRINT-94-49 *Contributed to the 4th European Particle Accelerator Conference (EPAC94), London, U.K., Jun 27 - Jul 1, 1994.*
- [71] E. Kikutani and Y. Minagawa, "Two tap digital filters for the KEK B bunch feedback systems," KEK-94-5.
- [72] E. Kikutani, T. Obina, T. Kasuga, Y. Minagawa, M. Tobiyama and L. Ma, "Frontend electronics for the bunch feedback systems for KEK B," KEK-PREPRINT-94-131 *Talk given at 6th Beam Instrumentation Workshop (BIW 94), Vancouver, Canada, 2-6 Oct 1994.*
- [73] E. Kikutani, T. Kasuga, Y. Minagawa, T. Obina and M. Tobiyama, "Recent progress in the development of the bunch feedback systems for KEK B," KEK-PREPRINT-95-20 *Contributed paper at 1995 Particle Accelerator Conference and International Conference on High-Energy Accelerators, 1 - 5 May, 1995, Dallas, Texas, U.S.A..*
- [74] E. Kikutani, M. Tobiyama and S. Kurokawa, "Development of a high-speed digital signal-process board for the KEK B bunch feedback systems," KEK-PREPRINT-96-49 *Talk given at 5th European Particle Accelerator Conference (EPAC 96), Sitges, Spain, 10-14 Jun 1996.*
- [75] E. Kikutani and M. Tobiyama, "Strategy for developing fast bunch feedback systems for KEKB," KEK-PREPRINT-97-14 *Talk given at 17th IEEE Particle Accelerator Conference (PAC 97): Accelerator Science, Technology and Applications, Vancouver, Canada, 12-16 May 1997.*
- [76] E. Kikutani and M. Tobiyama, "KEKB bunch feedback systems and related systems," KEK-PREPRINT-97-185 *Submitted at 3rd European Workshop on Beam Diagnostics and Instrumentation for Particle Accelerators (DIPAC 97), Frascati, Italy, 12-14 Oct 1997.*
- [77] E. Kikutani and Y. Minagawa, "Simulation study of feedback systems based on a two-tap FIR filter: Under beam-beam collisions," KEK-REPORT-98-1.
- [78] E. Kikutani, J. Flanagan and M. Tobiyama, "Limitations of multibunch feedback systems and extrapolation," KEK-PREPRINT-2000-045.
- [79]
- [79] S. Koscielniak and H. J. Tran, "Properties of a transverse damping system, calculated by a simple matrix formalism," TRI-PP-95-31 *Presented at 16th IEEE Particle Accelerator Conference (PAC 95) and International Conference on High Energy Accelerators (IUPAP), Dallas, Texas, 1-5 May 1995.*
- [80] G. Kraft *et al.*, "The Heavy ion therapy project at GSI," GSI-91-15.
- [81] J. L. Laclare, "Bunched Beam Instabilities," in *C80-07-07.43 LNS/044 To be given at 11th Int. Conf. on High Energy Accelerators, Geneva, Switzerland, Jul 7-11, 1980.*
- [82] J. L. Laclare, "Coasting beam transverse coherent instabilities," In **Jyvaeskylae 1992, Proceedings, General accelerator physics, vol. 1* 385-408. CERN Geneva - CERN-94-01 (94/01,rec.Mar.) 385-408.*
- [83] G. Lambertson, "Dynamic Devices: Pickups And Kickers," LBL-22085 *Presented at 5th U.S. Summer School on High Energy Particle Accelerators, Stanford, CA, Jul 15-26, 1985.*

-
- [84] G. Lambertson, "Bunch motion feedback for B factories," SLAC-AP-95 *Presented at B Factories: the State of the Art in Accelerators, Detectors, and Physics, Stanford, CA, 6-10 Apr 1992.*
- [85] G. Lambertson, "Beam bunch feedback," LBL-37764 *Prepared for 1994 US-CERN-Japan Joint Accelerator School: Topical Course: Frontiers of Accelerator Technology, Maui, HI, 3-9 Nov 1994.*
- [86] L. Ma, S. Kurokawa and E. Kikutani, "FIR filters for the bunch by bunch feedback system of TRISTAN-II," KEK-PREPRINT-93-22 *To be presented at 9th Symposium on Accelerator Science and Technology, Tsukuba, Japan, 25-27 Aug 1993.*
- [87] A. Mankofsky, "Three-Dimensional Electromagnetic Particle Codes And Applications To Accelerators," In **San Diego 1988, Proceedings, Linear accelerator and beam optics codes** 137-160. .
- [88] V. A. Melnikov, "Possibilities of technical implementation of nonlinear damping of transversal coherent oscillations of a beam," Nucl. Instrum. Meth. A **391** (1997) 93.
- [89] R.W. Miller, C.A. Ricci and R.J. Kansy, "An Acoustic Charge Transport Digitally Programmable Transversal Filter," *IEEE Journal of Solid-State Circuits, Vol.24, No. 6, pp.1675-1682, December 1989.*
- [90] R.W. Miller, R.J. Kansy, "Acoustic Charge Transport Digitally Programmable Transversal Filter 1990 *IEEE MTT-S Symposium Proceedings, cat #CH2848-0, Vol. 3, pp. 1111-1114, May 1990*
- [91] R.W. Miller, C.E. Nothnick and D.S. Bailey "Acoustic Charge Transport: Device technology and Applications," *Boston, USA: Artech House (1992) 570 p*
- [92] Y. Minagawa, E. Kikutani, M. Tobiyama and S. Kurokawa, "A systematic study of a transverse feedback system with a two-tap FIR filter," KEK-PREPRINT-96-50 *Talk given at 5th European Particle Accelerator Conference (EPAC 96), Sitges, Spain, 10-14 Jun 1996.*
- [93] Y. Minagawa, E. Kikutani, S. Kurokawa and M. Tobiyama, "Study of transverse bunch-by-bunch feedback systems based on the two tap FIR filter," Nucl. Instrum. Meth. **A416** (1998) 193.
- [94] L. Palumbo, V. G. Vaccaro and M. Zobov, "Wake Fields and Impedance," LNF-94-041-P, Sep 1994. 70pp.
- [95] S. Prabhakar *et al.*, "Observation and modal analysis of coupled-bunch longitudinal instabilities via a digital feedback control system," Part. Accel. **57** (1997) 175.
- [96] J. T. Rogers *et al.*, "Operation of a fast digital transverse feedback system in CESR," In **Dallas 1995, PAC, vol. 4* 2426-2428.*
- [97] R. Rojko and U. Blell "A transverse feedback system (TFS) for the Heavy Ion Synchrotron (SIS) at the GSI," *Proceeding of EPAC2000, Vienna, 2000, 1927-1929.*
- [98] G. Rumolo, "Theory of transverse instabilities of coasting beams in accelerator rings," *GSI-Interner Bericht, GSI-HSB-98-1, 20 p..*
- [99] J. Rossbach and P. Schmuser, "Basic course on accelerator optics," In **Jyvaeskylae 1992, Proceedings, General accelerator physics, vol. 1* 17-88. CERN Geneva - CERN-94-01 (94/01,rec.Mar.) 17-88.*
- [100] G. Sabbi, "Simulation of coupled oscillator feedback systems counteracting the strong head - tail effect in LEP," CERN-SL-96-02-AP.

-
- [101] L. Sapozhnikov, J. D. Fox, J. J. Olsen, G. Oxoby, I. Linscott, A. Drago and M. Serio, "A longitudinal multibunch feedback system using parallel digital signal processors," SLAC-PUB-6365 *Workshop on Beam Instrumentation, Santa Fe, NM, 20-23 Oct 1993*.
- [102] U. Schaaf, "Schottky-Diagnose und BTF-Messungen an gekühlten Strahlen im Schwerionen-Speicherring ESR," *Dissertation Universität Frankfurt, GSI 91-22 (GSI Darmstadt, 1991)*.
- [103] M. Serio and M. Zobov, "Measurement of transverse and longitudinal spectra," LNF-93-042-P *Invited talk at 1st European Workshop on Beam Instrumentation and Diagnostics for Particle Accelerators, Montreux, Switzerland, 3-5 May 1993*.
- [104] M. Serio *et al.*, "Multibunch instabilities and cures," in *NONE LNF-96-033-PC Prepared for 5th European Particle Accelerator Conference (EPAC 96), Sitges, Spain, 10-14 Jun 1996*.
- [105] J. D. Simpson and R. Konecny, "Low Dispersion Notch Filter For Multi - Ghz Frequencies Using Fiber Optics Delays," ANL-HEP-CP-85-42 *Presented at 1985 Particle Accelerator Conf., Vancouver, B.C., Canada, May 13-16, 1985*.
- [106] S. R. Smith, "Beam position monitor engineering," SLAC-PUB-7244 *Talk given at 7th Beam Instrumentation Workshop (BIW 96), Argonne, IL, 6-9 May 1996*.
- [107] M. Stampfer, "Development of an Active Feedback System to Damp Transverse Coherent *Diplomarbeit, Max-Planck-Institut für Kernphysik, Heidelberg, 1992*.
- [108] M. Steck, "Design of the electron cooling system for SIS," *Darmstadt GSI - GSI-Nachr.-95-12 (95,rec.Jan.96) 25-26*.
- [109] J. M. Steimel and D. McGinnis, "Damping in the Fermilab booster," *Prepared for 1993 IEEE Particle Accelerator Conference (PAC 93), Washington, DC, 17-20 May 1993*.
- [110] J. M. Steimel, "Fast digital dampers for the Fermilab booster," *In *Dallas 1995, PAC, vol. 4* 2384-2388*.
- [111] P. Strehl and H. Vilhjalmsson, "The SIS-beam diagnostic system," *pp. 1413-1415*.
- [112] "TMS320C6000 Peripherals Reference Guide," *TEXAS INSTRUMENTS, Literature Number: SPRU190C, 1999 477 p.*
- [113] "TMS320C6000 Assembly Language Tools User's Guide," *TEXAS INSTRUMENTS, Literature Number: SPRU186E, 1999 386 p.*
- [114] "TMS320C6000 Optimizing C Compiler User's Guide," *TEXAS INSTRUMENTS, Literature Number: SPRU187E, 1999 387 p.*
- [115] "TMS320C6000 CPU and Instruction Set Reference Guide," *TEXAS INSTRUMENTS, Literature Number: SPRU189D, 1999 391 p.*
- [116] "TMS320C6000 Board Design for JTAG," *TEXAS INSTRUMENTS, Application report: SPRA584, 1999 7 p.*
- [117] "TMS320C620x/TMS3206701 DMA and CPU: Data Access Performance," *TEXAS INSTRUMENTS, Application report: SPRA614, 1999 28 p.*
- [118] "Code Composer Studio User's Guide," *TEXAS INSTRUMENTS, Literature Number: SPRU328A, 1999 234 p.*
- [119] D. Teytelman *et al.*, "Feedback control and beam diagnostic algorithms for a multiprocessor DSP system," SLAC-PUB-7305 *Talk given at 7th Beam Instrumentation Workshop (BIW 96), Argonne, IL, 6-9 May 1996*.

-
- [120] D. Teytelman *et al.*, “Operation and performance of a longitudinal feedback system using digital signal processing,” SLAC-PUB-6675 *Presented at 6th Beam Instrumentation Workshop (BIW 94), Vancouver, Canada, 2-6 Oct 1994.*
- [121] M. Tobiyama, E. Kikutani and Y. Minagawa, “Longitudinal bunch feedback system with a two tap FIR filter prototype,” KEK-PREPRINT-95-103 *Contributed to 10th Symposium on Accelerator Science and Technology, Hitachinaka, Japan, 25-27 Oct 1995.*
- [122] M. Tobiyama, E. Kikutani, T. Taniguchi and S. Kurokawa, “Development of a two tap FIR filter for bunch by bunch feedback systems,” KEK-PREPRINT-95-104 *Contributed to 10th Symposium on Accelerator Science and Technology, Hitachinaka, Japan, 25-27 Oct 1995.*
- [123] M. Tobiyama and E. Kikutani, “Study of bunch by bunch feedback system in TRISTAN-AR,” KEK-PREPRINT-97-13 *Talk given at 17th IEEE Particle Accelerator Conference (PAC 97): Accelerator Science, Technology and Applications, Vancouver, Canada, 12-16 May 1997*
- [124] M. Tobiyama and E. Kikutani, “Bunch-by-bunch feedback systems for KEKB rings,” KEK-PREPRINT-98-8 *Talk given at 1st Asian Particle Accelerator Conference (APAC 98), Tsukuba, Japan, 23-27 Mar 1998.*
- [125] M. Tobiyama and E. Kikutani, “Commissioning of KEKB bunch feedback systems,” KEK-PREPRINT-99-4 *The 1999 particle accelerator conference (PAC’99) Mar 29 - Apr 2, 1999, New York City, New York, U.S.A..*
- [126] M. Tobiyama, E. Kikutani and J. W. Flanagan, “Bunch by bunch feedback systems for KEKB rings,” KEK-PREPRINT-99-71 *In *Wako 1999, Accelerator science and technology* 555-557.*
- [127] M. Tobiyama and E. Kikutani, “Development of a high speed digital signal process system for bunch-by-bunch feedback systems,” *Phys. Rev. ST Accel. Beams* **3** (2000) 012801.
- [128] T. Toifl, “Integrated circuits for the synchronisation of high-energy physics experiments,” *Dissertation CERN, Genf 1999.*
- [129] L. Vos, “Transverse emittance blow-up from dipole errors in proton machines,” CERN-LHC-PROJECT-REPORT-193 *Presented at 6th European Particle Accelerator Conference (EPAC 98), Stockholm, Sweden, 22-26 Jun 1998.*
- [130] T. Weiland and R. Wanzenberg, “Wake fields and impedances,” DESY-M-91-06, May 1991. 54pp.
- [131] H. Wiedemann, “Particle accelerator physics: Basic principles and linear beam dynamics,” *Berlin, Germany: Springer (1993) 445 p.*
- [132] H. Wiedemann, “Particle accelerator physics: 2: Nonlinear and higher order beam dynamics,” *Berlin, Germany: Springer (1995) 464 p.*
- [133] E. Wilson, “Transverse beam dynamics,” *In *Jyvaeskylae 1992, Proceedings, General accelerator physics, vol. 1* 131-158. CERN Geneva - CERN-94-01 (94/01,rec.Mar.) 131-158.*
- [134] “Speed Metrics For High-Performance FPGAs,” *XILINX Application Brief XBRF015, 1997 10 p.*
- [135] “XCR3320: 320 Macrocell SRAM CPLD,” *XILINX Product specification DS033, 2000 43 p.*

- [136] J. Xu, J. Claus, E. Raka, A. G. Ruggiero and T. J. Shea, "The Transverse damper system for RHIC," BNL-45356 *Presented at 1991 IEEE Particle Accelerator Conf., San Francisco, CA, May 6-9, 1991.*
- [137] V. M. Zhabitsky, I. L. Korenev and L. A. Yudin, "The Resistive instability damper system for the first stage of the UNK accelerator with IIR filter in feedback," JINR-P9-91-494.
- [138] V. M. Zhabitsky, "Transverse feedback system with a digital filter," Nucl. Instrum. Meth. **A391** (1997) 96.
- [139] B. Zotter and F. Sacherer, "Transverse Instabilities Of Relativistic Particle Beams In Accelerators And Storage Rings," In **Erice 1976, Proceedings, International School Of Particle Accelerators (CERN 77-13)*, Geneva 1977, 175-218.*

Acknowledgements

I cordially acknowledge Prof. H. L. Hartnagel for supervising my dissertation and continuous help I received from him during my stay at the Technical University Farmstead as well as for his kindly offered financial support during all three years.

My special gratitude goes also to Dr. N. Angert for being a co-supervisor of my thesis. He kindly offered me financial support during my last six months at GSI.

I am especially indebted to Dr. U. Blell, who gave me infinite support and encouragement during my stay at GSI. Special thanks for Dr. K. Beilenhoff and Dr. H. Eickhoff, who were giving me support from the beginning of my work.

My coming to Germany was possible very much due to the help and support of Prof. J. Jasenek, who introduced me to Prof. H.L.Hartnagel at Summer School, Bratislava, in 1997. I am very grateful to him for making this chance to become a reality.

A very special place in my thanksgivings I have to reserve for Dr. K. Beckert, Dr. K. Blasche, Dr. O. Boine-Frankenheim, Dr. B. Franzke, R. Menges, Dr. F. Nolden, Dipl.-Ing. P. Moritz, Dr. M. Steck, and Dipl.-Ing. A. Schwinn. I appreciate their help and support during my measurements and first tests with the automatic feedback system in SIS as well as in ESR.

For the numerous advises and consultations especially connected with the signal processing system, measurements and putting both cards into operation in a laboratory environment, I also would like to thank Dipl.-Ing. A. Badura, Dipl.-Ing. A. Franke, J. Gross, Dipl.-Ing. G. Englert, Dipl.-Ing. R. Hartmann, Dipl.-Ing. J. Hoffmann, and Dipl.-Ing. W. Panschow.

My gratitude also goes to all colleagues at the Institute of Microwave Engineering for their valuable discussions and suggestions as well as providing great encouragement.

Additionally I would like to thank Dipl.-Phys. B. Franczak and Dipl.-Ing. P. Keinberger for their help with software preparation and for their assistance concerning on NODAL program.

Thanks to G. Eidmann, Dipl.-Ing. G. May, W. Meufels, and S. Voltz for help with questions on connection diagrams and layout preparation. Without their support it would not be possible to realise both printed circuit boards in such a short time.

For the friendly environment at GSI and for their help, I would like to thank Dr. R. C. Bär, Dr. G. Franchetti, Dr. G. Rumolo, and Dipl.-Phys. Liu.

I want to express my gratitude to Dr. R. C. Bär, Dr. U. Blell, Dr. V. Ichizli, Dipl.-Ing. A. Megej and all those who read this manuscript and made helpful suggestions.

Because the largest part of this thesis was carried out as part of the GSI project I would like to thank all other not mentioned here co-workers of GSI for a fruitful collaboration and their excellent technical support.

Finally, I want to thank my family for their unconditional support. To them I dedicate this work.

Lebenslauf

Persönliche Daten

Name: Roman Rojko
Adresse: Hurbanova 18/137
916 01 Stará Turá, Slowakei
Geburtsdatum: 11. September 1971
Geburtsort: Trenčín, Slowakei
Staatsangehörigkeit: slowakisch
Familienstand: ledig

Ausbildungsdaten und Berufsweg

Schule:	1978–1986	Grundschule, Stará Turá.
	1986–1990	Gymnasium, Nové Mesto nad Váhom. Abschluß: Abitur.
Studium:	1990–1995	Technische Universität Bratislava, Studiengang Elektrotechnik, Fachrichtung Mikroelektronik.
	1. Juni 1995	Abschluß: Dipl.-Ing. an der TU-Bratislava.
	1995–1996	Entwicklungsabteilung/Projekt-Ingenieur, Chirana-Medical, AG, Slowakei
	1996–1997	Berater/Softwareentwickler, HMH, GmbH., Bratislava, Slowakei
	seit 1998	Doktorand am Institut für Hochfrequenztechnik der Technischen Universität Darmstadt
	1998–2001	Doktorarbeit, durchgeführt bei der Gesellschaft für Schwerionenforschung mbH in Darmstadt.
	1. Juni 2001	IT-Berater, ESPRiT Unternehmensberatung, AG in München

Darmstadt, den 12. November 2002